united nations
educational, scientific
and cultural
organization

international atomic
energy agency

the
abdus salam
international centre for theoretical physics

COURSE ON CLIMATE VARIABILITY
STUDIES IN THE OCEAN
"Tracing & Modelling the Ocean Variability"
16 - 27 June 2003

301/1507-2

Thermohaline Circulation and Climate

Edward Sarachik
University of Washington
Seattle, USA

Please note: These are preliminary notes intended for internal distribution only.

THERMOHALINE CIRCULATION AND CLIMATE

E.S. SARACHIK
UNIVERSITY OF WASHINGTON
sarachik@atmos.washington.edu

THERMOHALINE CIRCULATION AND CLIMATE

1. Some Basics

Observations

Density

Mass and Heat Capacity of Ocean

Wind Driven and Thermohaline Circulations

NADW vs. AABW

Intermediate Waters

2. Atlantic THC

Role in Global Climate

Paleo Variability

Modern Variability

3. Modeling the Thermohaline Circulation

NADW ON

NADW OFF

4. The Connection Between the Northern and Southern Branches of the THC

5. Thermohaline Variability

Multiple Equilibria

Stochastic Forcing

Oscillatory Behavior

6. Thermohaline Circulation and Global Warming

1. Ocean Basics

✵ Some Numbers

Mass of Water: 1 Tonne /m^3

Mass of Atmospheric Column/m^2 = 10 tonne/m^2

Top 10 m of ocean = 10 tonne /m^2

∴ Top 2.5 m of ocean has same heat capacity as entire atmospheric column above it.

1 Sv. = 1,000,000 m^3/sec of water

Rainfall Rate on Earth ~ 3 mm/day ~ 16 Sv.

Volume of Ocean = 1.37 x 10^{18} m^3

✵ Equation of State of Sea Water

Role of Salinity at Low Temperatures

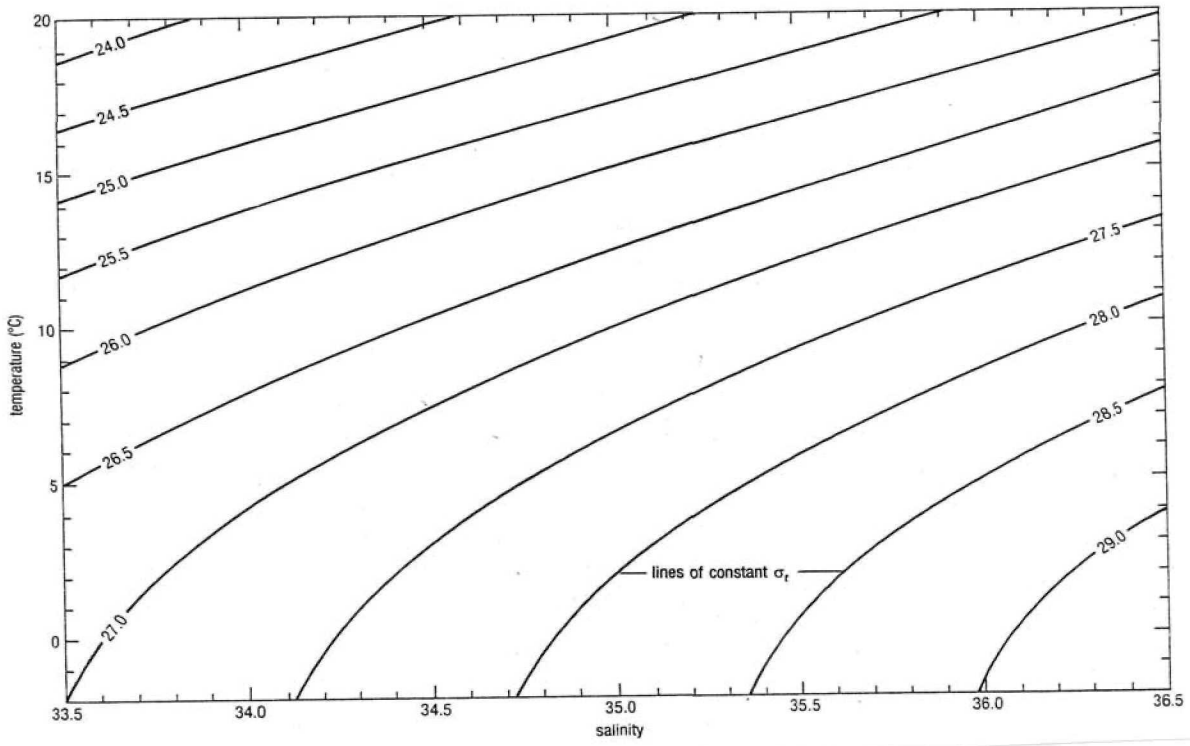

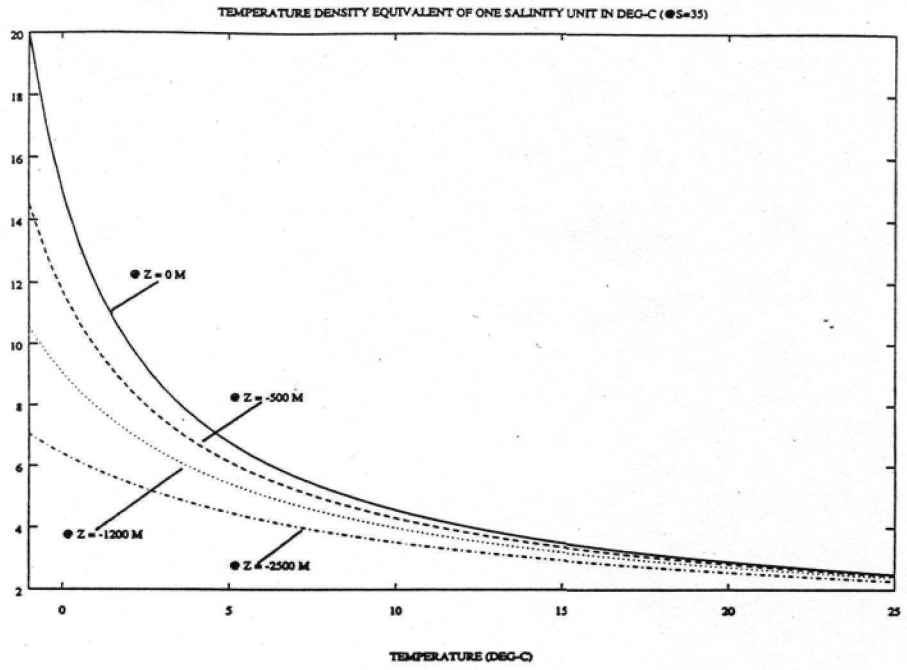

Figure 5.17: The number of °C that are the density equivalent of a single salinity unit as a function of temperature at the surface (solid), 500 m depth (dashed), 1200 m depth (dotted), and 2500 m depth (dash-dotted). The UNESCO formula for the equation of state was used to make this plot.

The Observational Situation

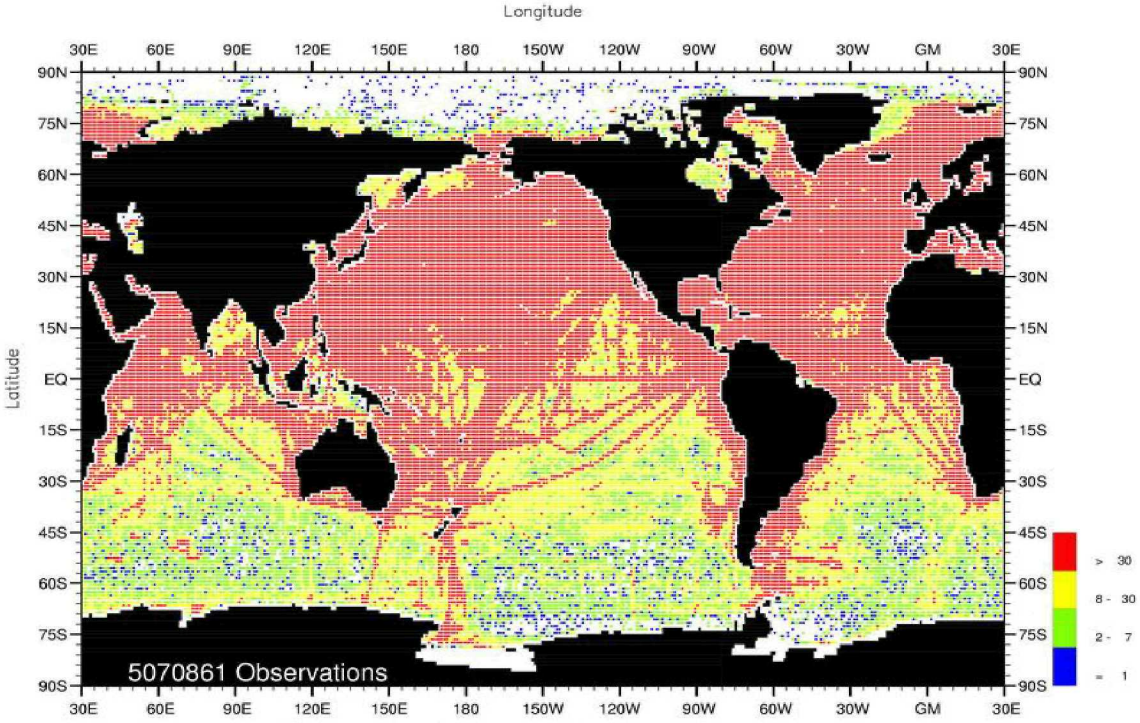

Fig. A1-1. Annual temperature observations at the surface.

World Ocean Atlas 2001
Ocean Climate Laboratory/NODC

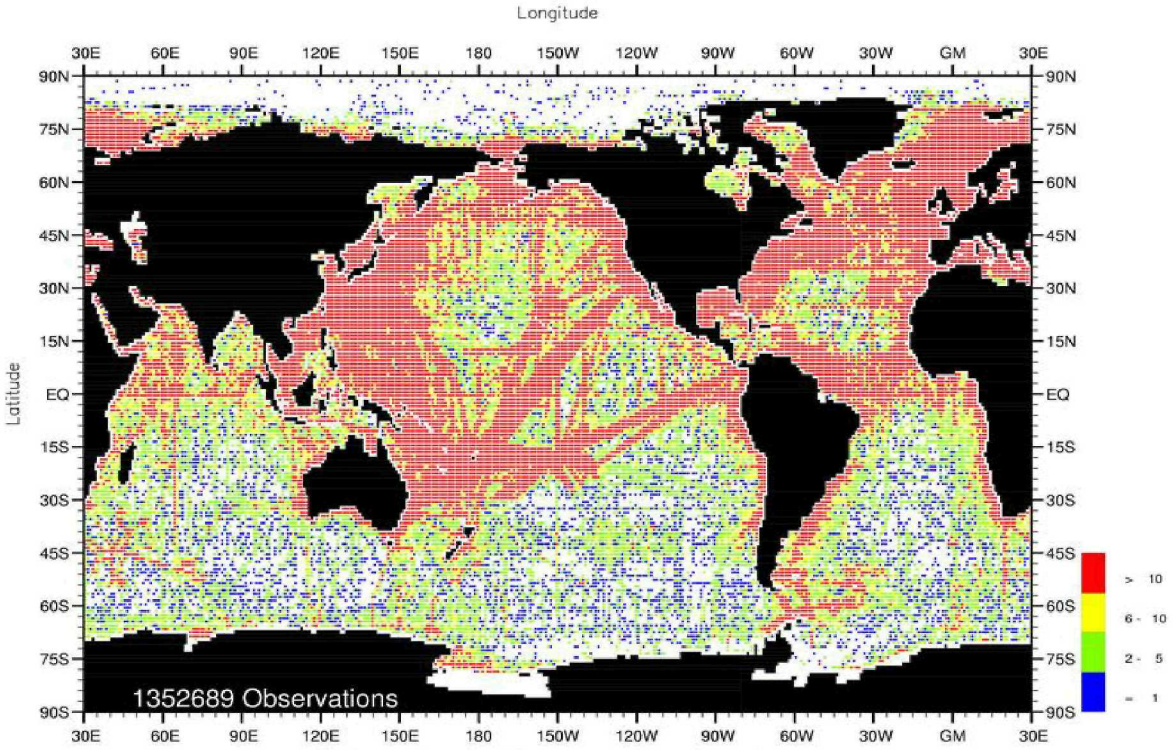

Fig. A1-1. Annual salinity observations at the surface.

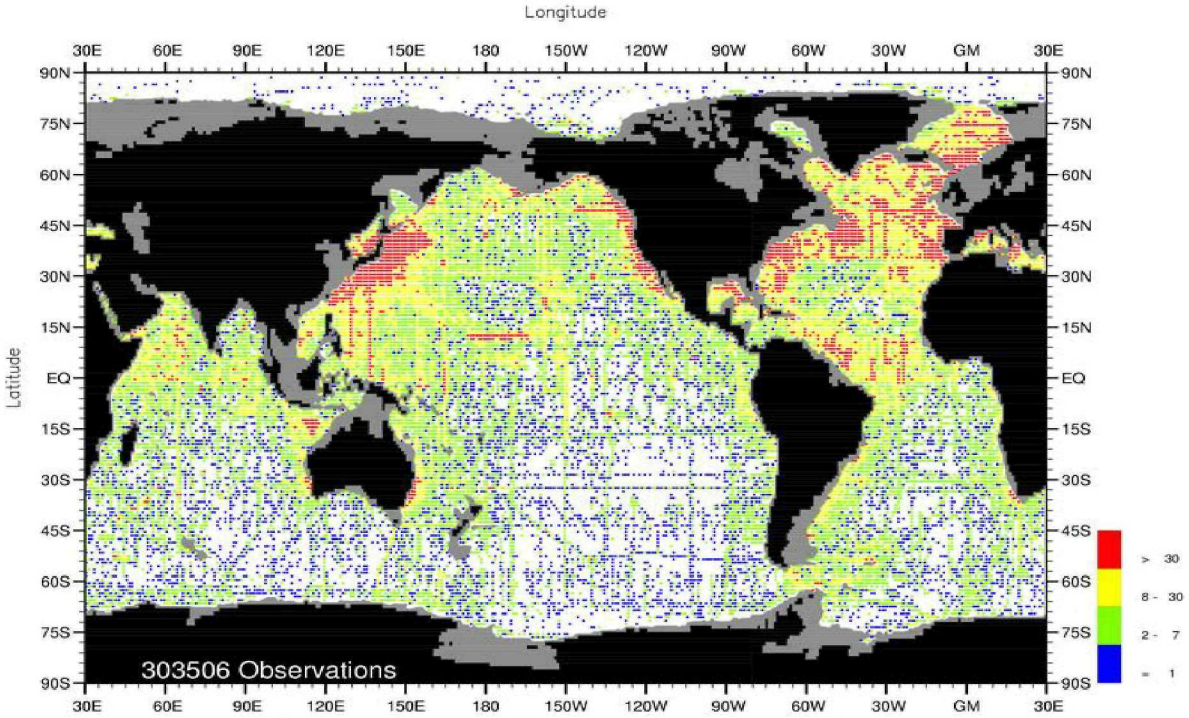

Fig. A1-19. Annual temperature observations at 1000 m. depth.

World Ocean Atlas 2001
Ocean Climate Laboratory/NODC

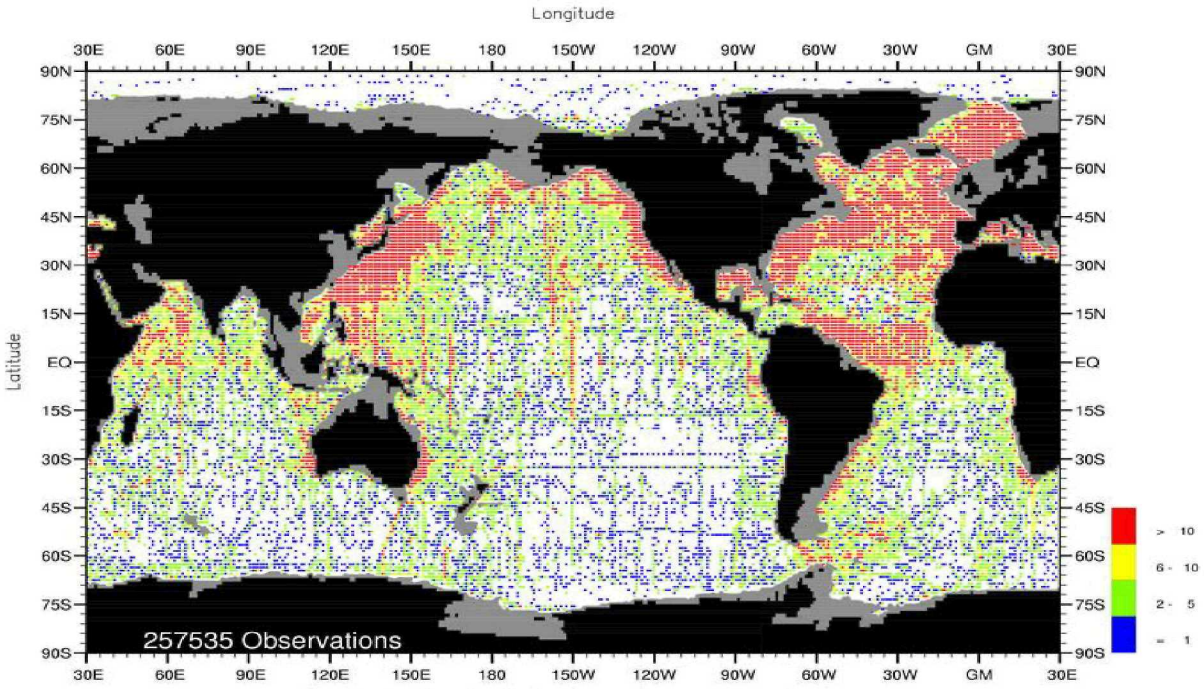

Fig. A1-19. Annual salinity observations at 1000 m. depth.

World Ocean Atlas 2001
Ocean Climate Laboratory/NODC

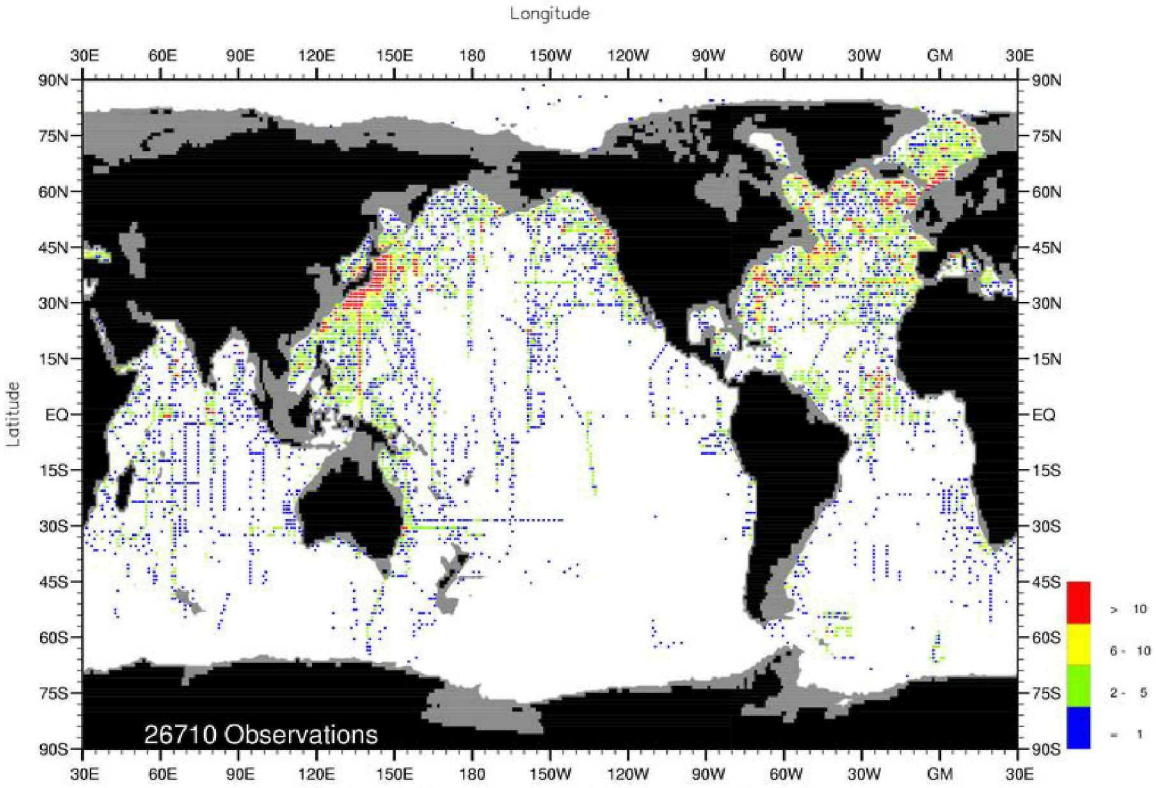

Fig. L1-19. July salinity observations at 1000 m. depth.

World Ocean Atlas 2001
Ocean Climate Laboratory/NODC

[A good place to look for data and maps from the World Ocean Atlas 1998 is: http://www.nodc.noaa.gov/OC5/]

Data can be downloaded and/or plotted at: http://ferret.wrc.noaa.gov/Ferret/LAS/LAS_servers.html

Density at Ocean Surface

Difference Between Atlantic & Pacific

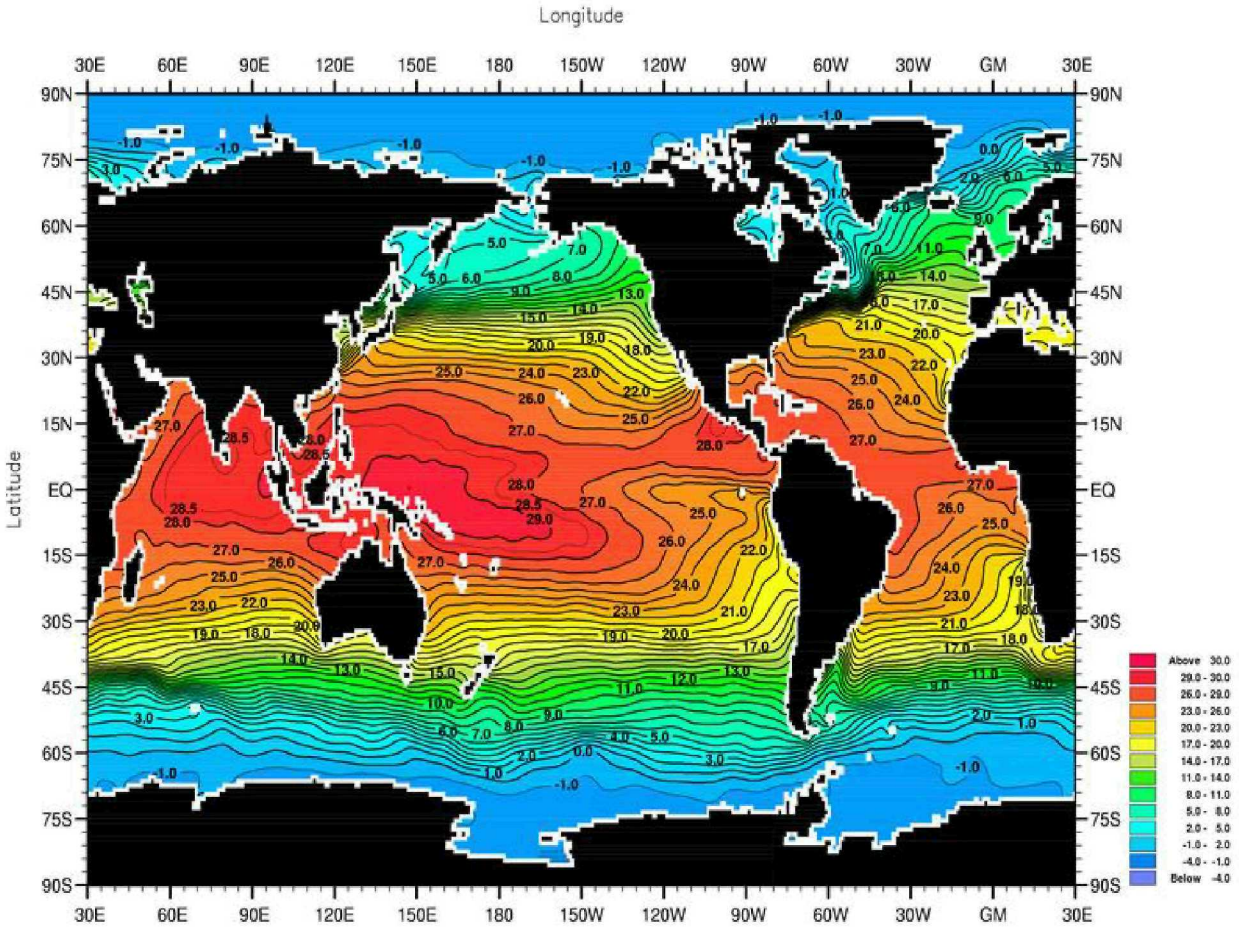

Fig. A2-1. Annual mean temperature (°C) at the surface.

Minimum Value= -1.93 Maximum Value= 29.93 Contour Interval: 1.00

World Ocean Atlas 2001
Ocean Climate Laboratory/NODC

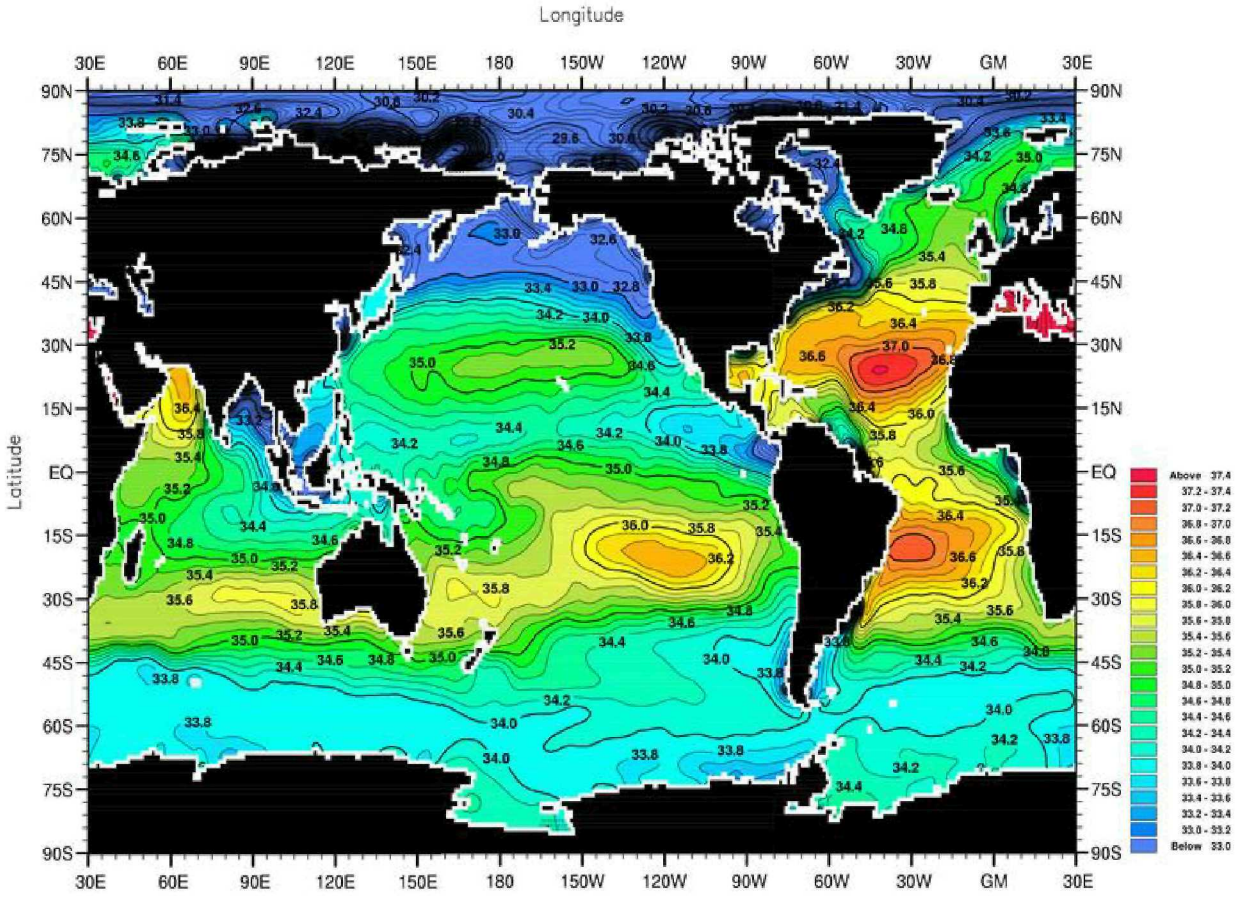

Fig. A2-1. Annual mean salinity (PSS) at the surface.

Minimum Value= 2.37 Maximum Value= 40.37 Contour Interval: 0.20

World Ocean Atlas 2001
Ocean Climate Laboratory/NODC

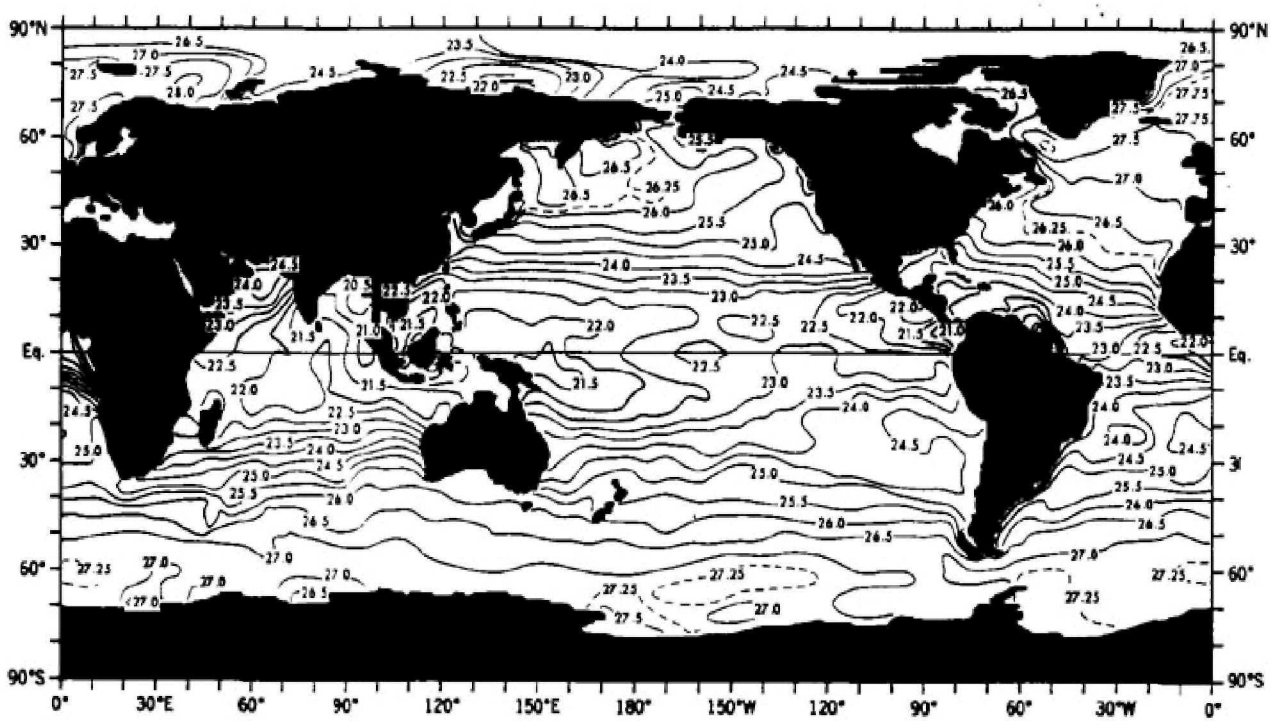

NH Winter

Density

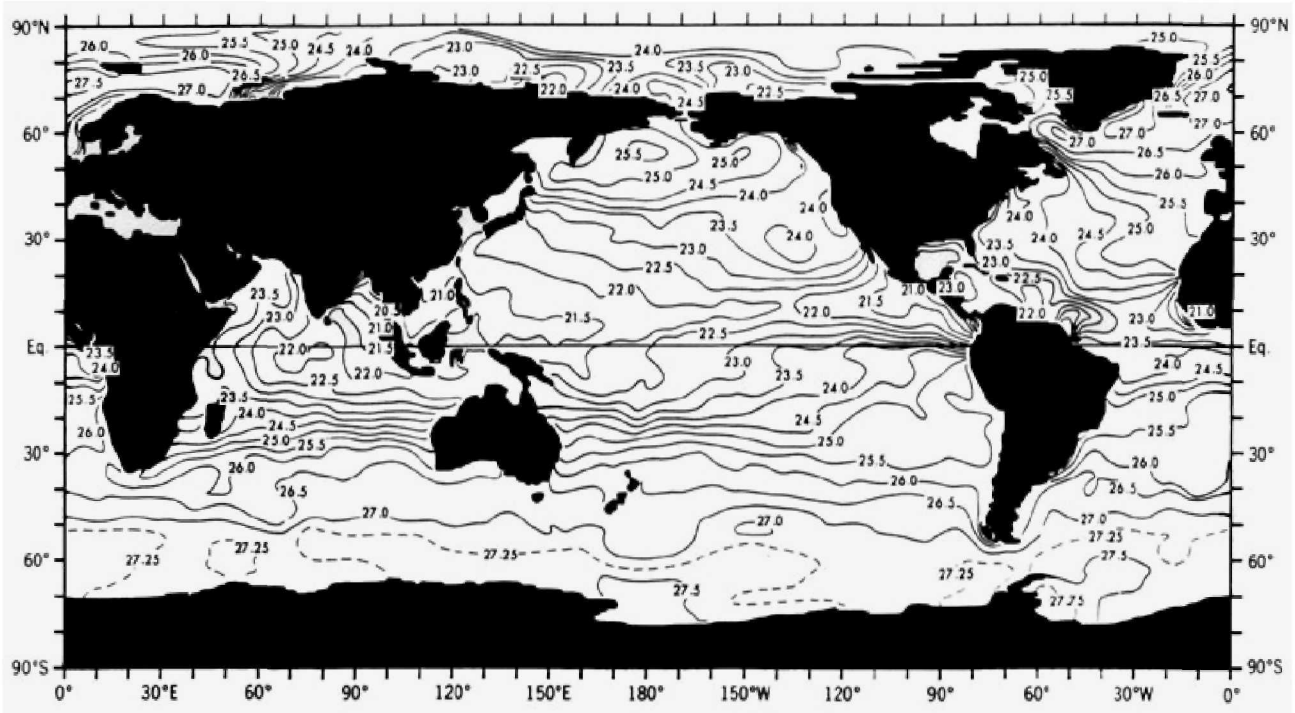

NH Summer

Ocean Stratification

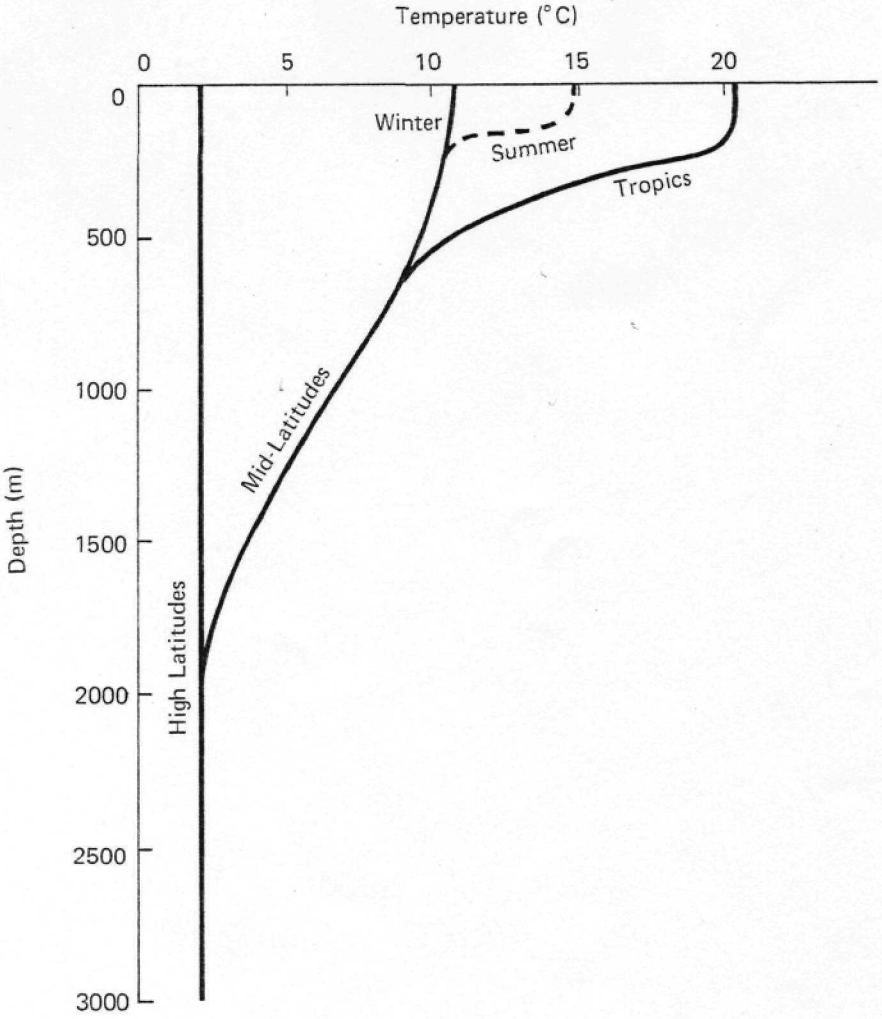

Figure 1.3. Typical temperature profiles in the open ocean.

Currents

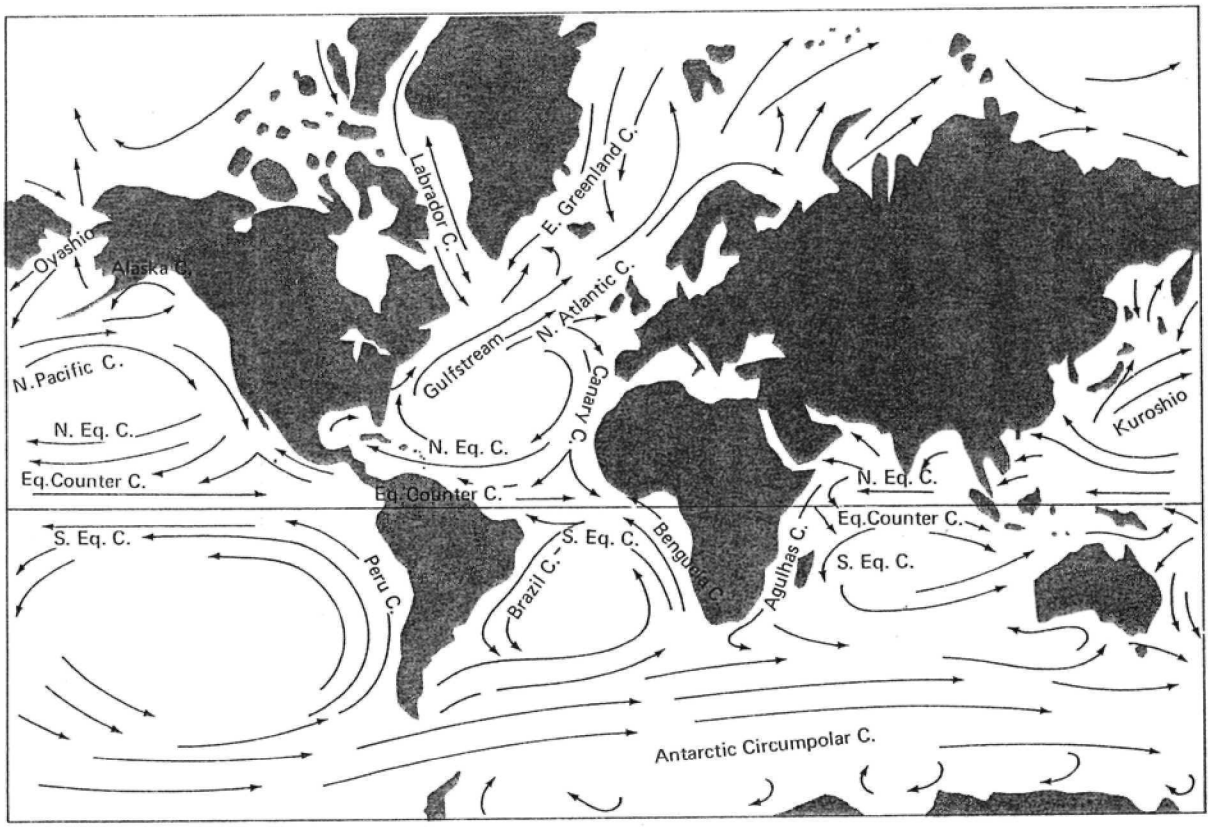

Figure 8.1. Major surface currents of the world oceans.

✵ Convection and Mean Sinking

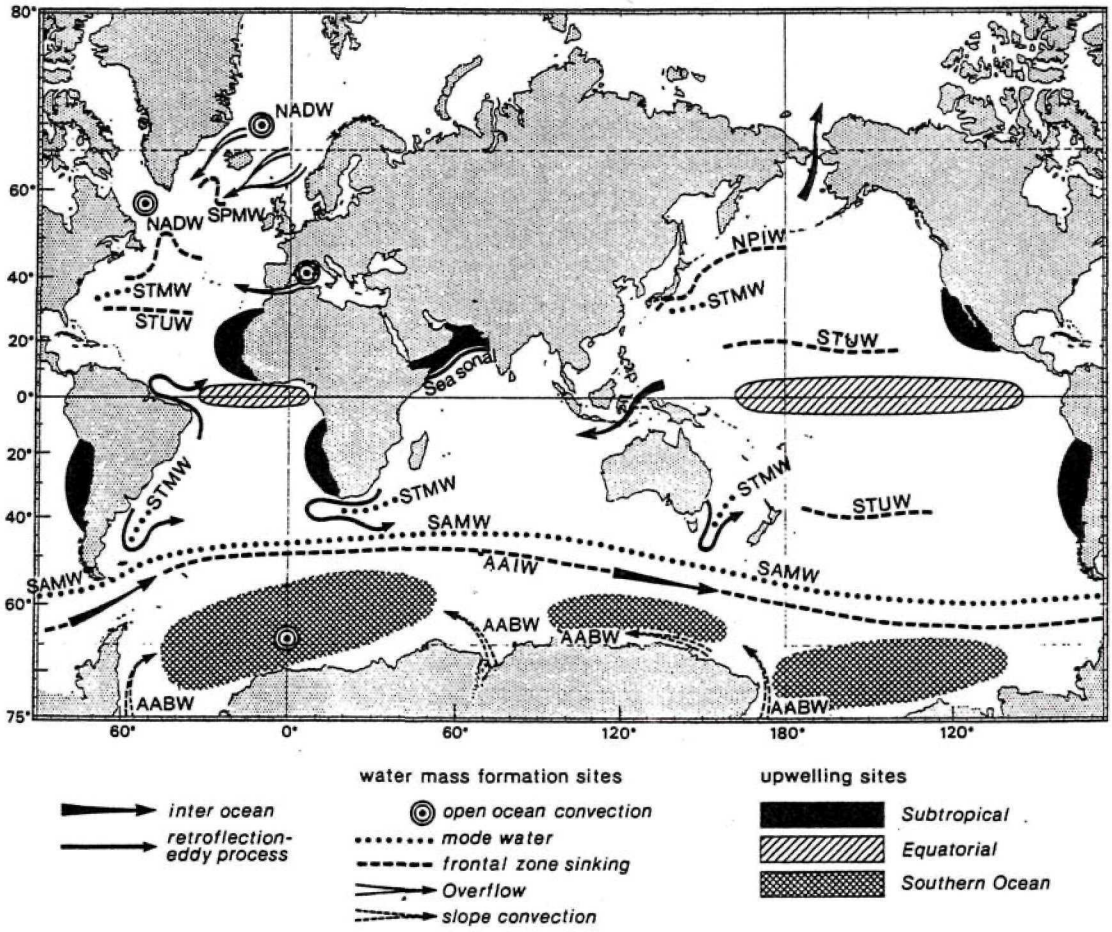

- Location of generation and transformation areas of the major water masses: North Atlantic Deep Water (NADW), Antarctic Bottom Water (AABW), Subtropical Model Water (SAMW), Subtropical Underwater (STUW), Subpolar Mode Water (SPMW) and North Pacific Intermediate Water (NPIW); also indicated are interocean and intergyre exchange/retroflection regimes. The dashed line in the southern ocean circumpolar belt marks the polar front and the formation region for Antarctic Intermediate water (AAIW). In the regions where STUW forms, it produces the sub-surface salinity maximum.

2. The Atlantic Thermohaline Circulation

- **Role in the Global Climate:**

  Surface Temperature Gradients

  Heat Flux to Atmosphere

  Maintenance of Equatorial Thermocline

  ENSO

  Variability of All of Above

Heat fluxes to the ocean

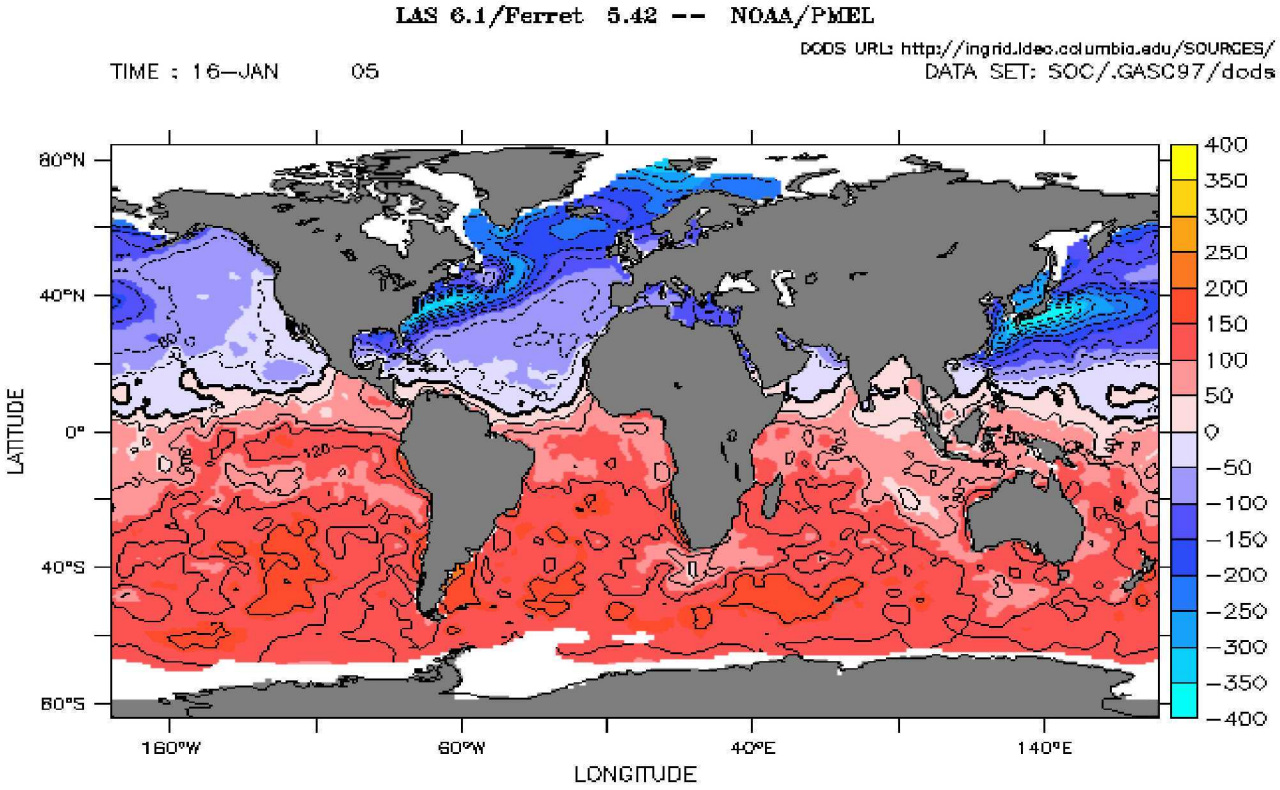

Net heat flux (positive for heat gain by the ocean) (W/m2)

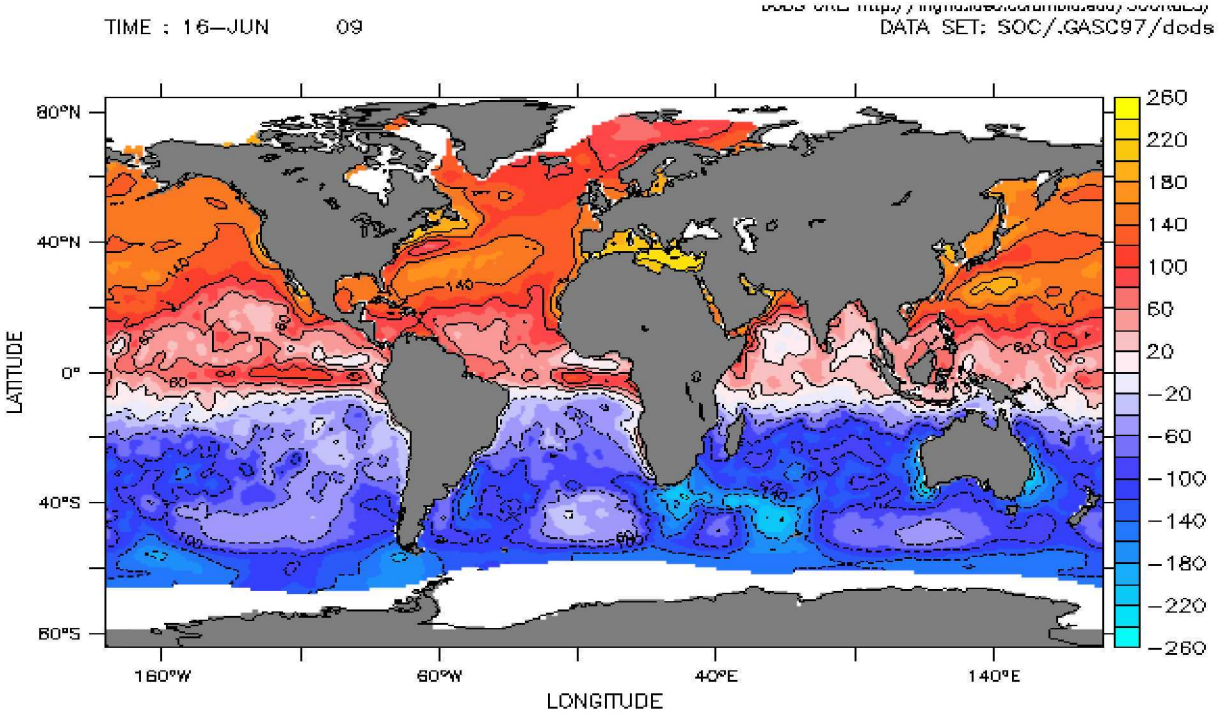

Net heat flux (positive for heat gain by the ocean) (W/m2)

Ocean Transports

Heat

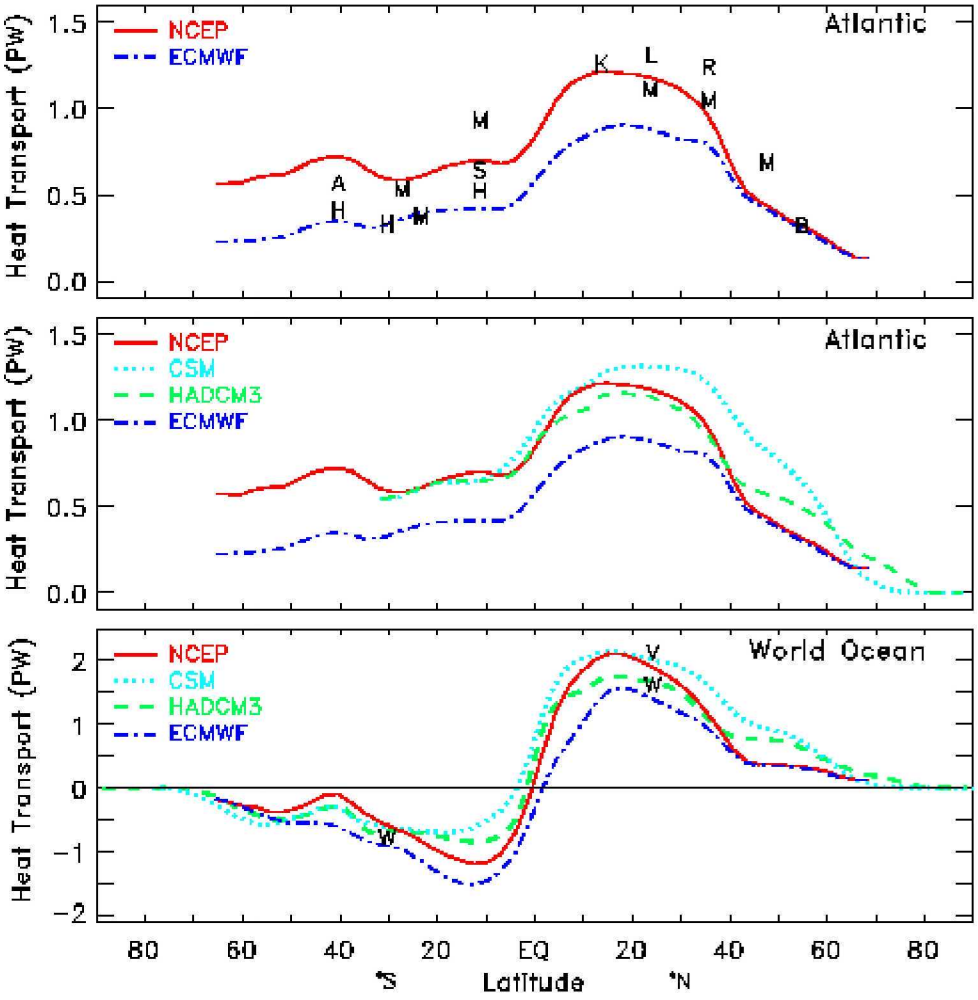

Fresh Water

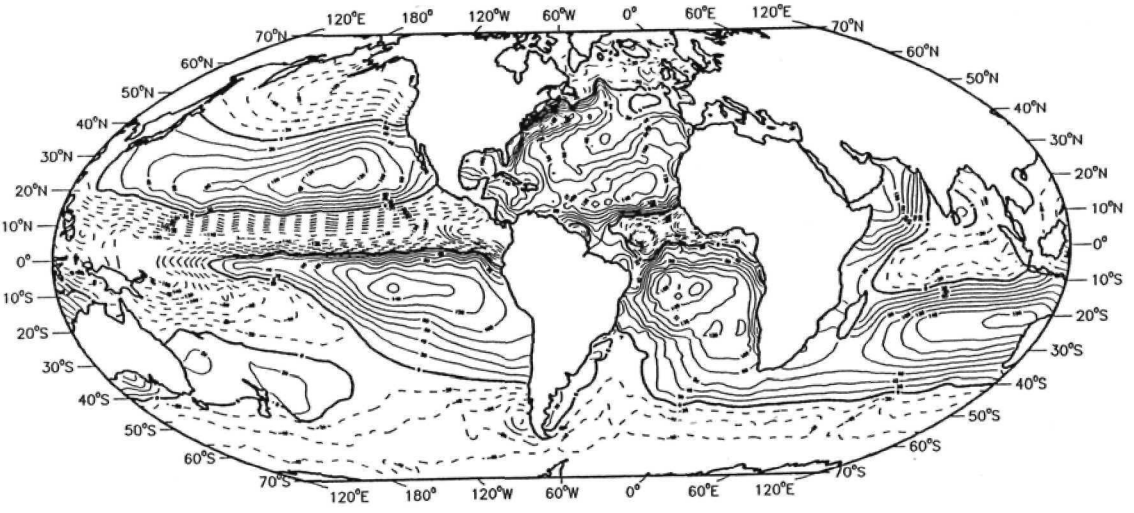

Figure 2. A map of evaporation minus precipitation (E-P) over the global ocean, in centimeters per year. This is a composite of Schmitt et al. (1989) for the Atlantic and Baumgartner and Reichel (1975) for the other oceans. The contour interval is 20 cm/yr and the dashed lines indicate net precipitation.

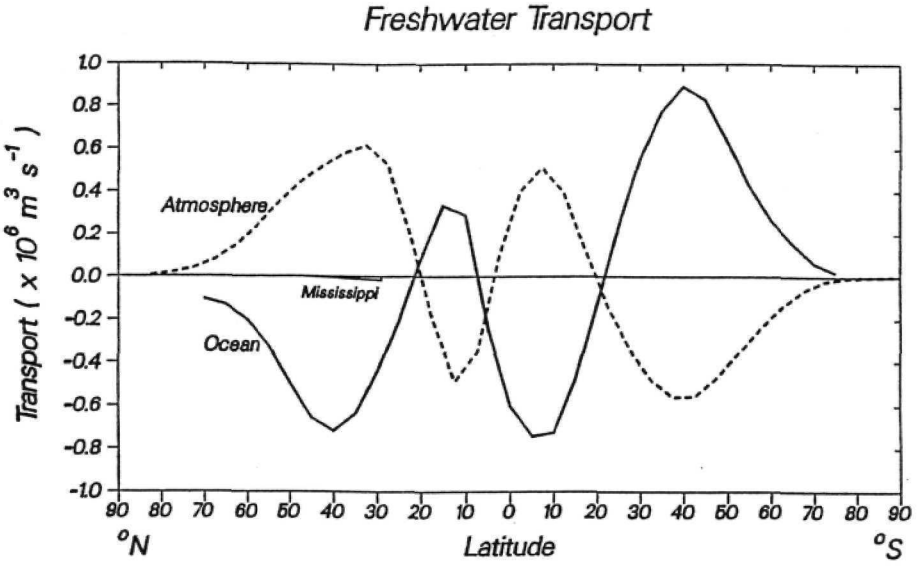

Figure 4. Meridional transport of water by the global ocean and atmosphere, in Sverdrups. The oceanic estimate derives from the integration of the E-P value shown in Fig. 2, plus river discharges into the ocean. The actual meridional transports by rivers alone is small; an estimate for the Mississippi is shown. The atmospheric transport of water vapor comes from Peixoto and Oort (1983).

✵ Water Masses

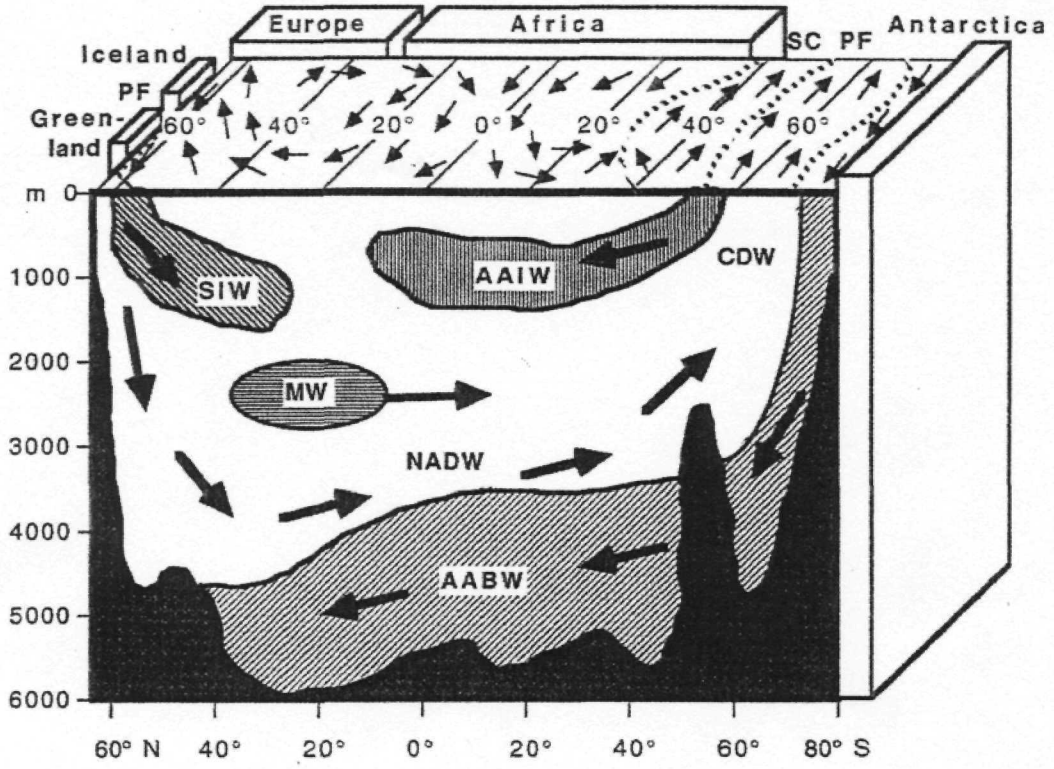

FIGURE 1 Schematic of water-mass distribution in the Atlantic (updated from Dietrich and Ulrich, 1968). AABW: Antarctic Bottom Water; NADW: North Atlantic Deep Water; CDW: Circumpolar Deep Water; SIW: Sub-Arctic Intermediate Water; AAIW: Antarctic Intermediate Water; MW: Mediterranean Water; PF: Polar Front; SC: Subtropical Convergence.

Salinity of High Latitudes: Effect on Sea Ice

Strength of the Gulf Stream and Brazil Current

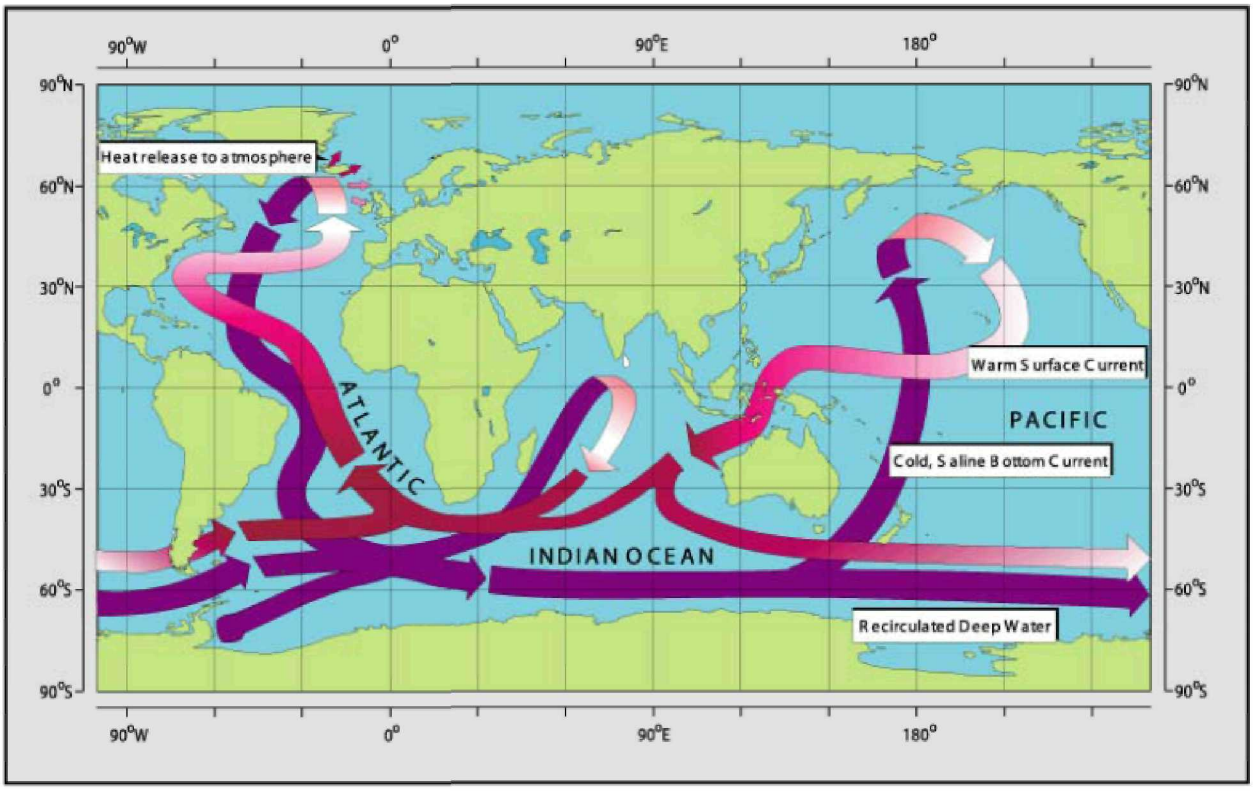

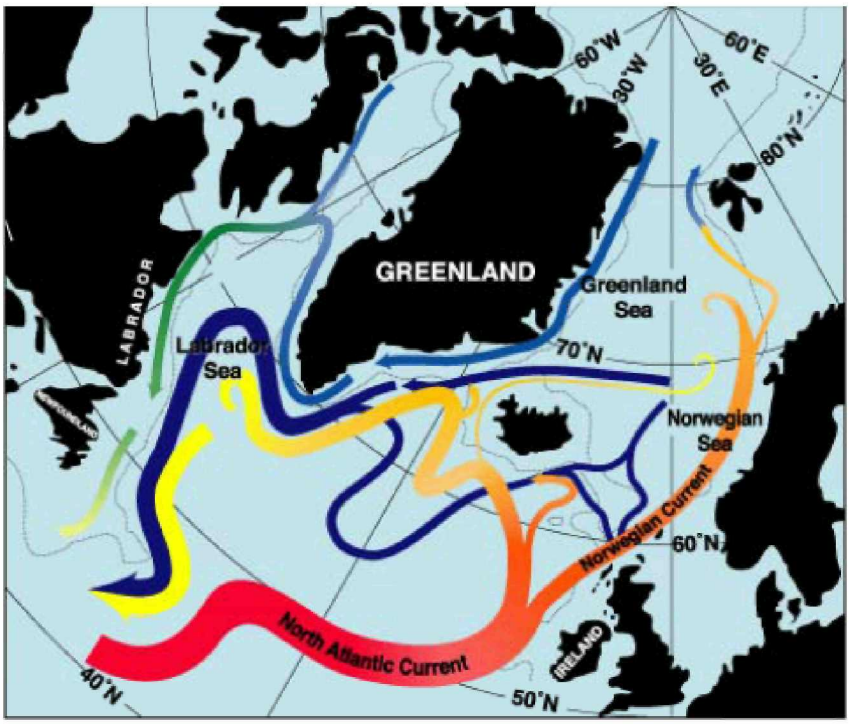

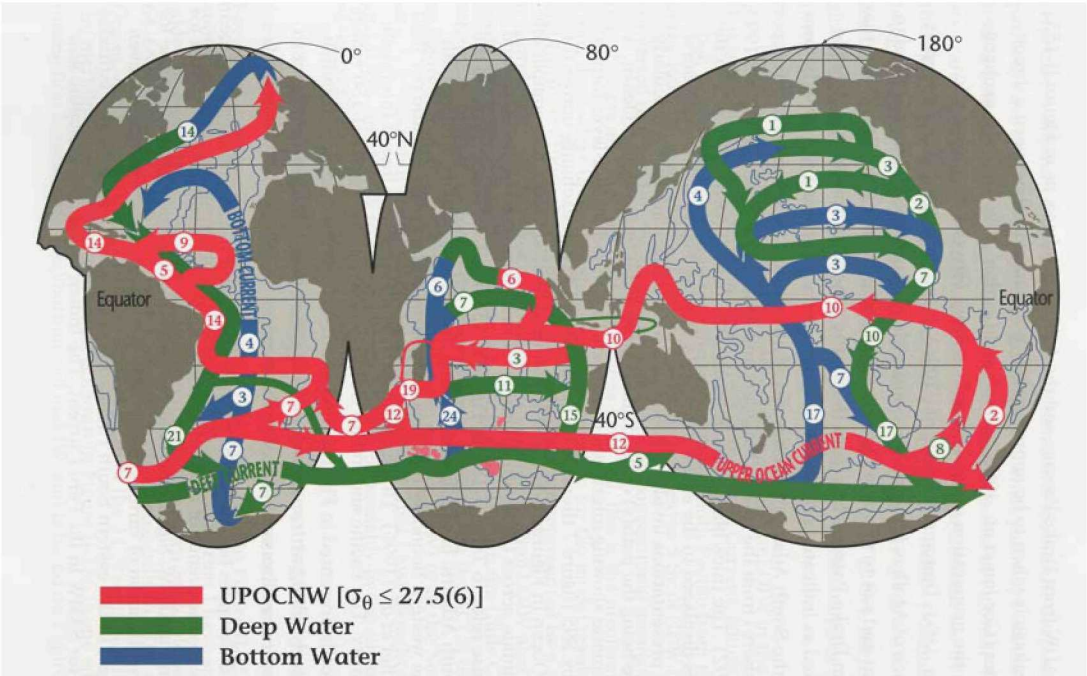

Figure II-156: An update of the 3-layer global interbasin exchange summary by S95, figure 9 there. Blue represents bottom water, green deep, and red the upper ocean. Transports in Sverdrups in circles.

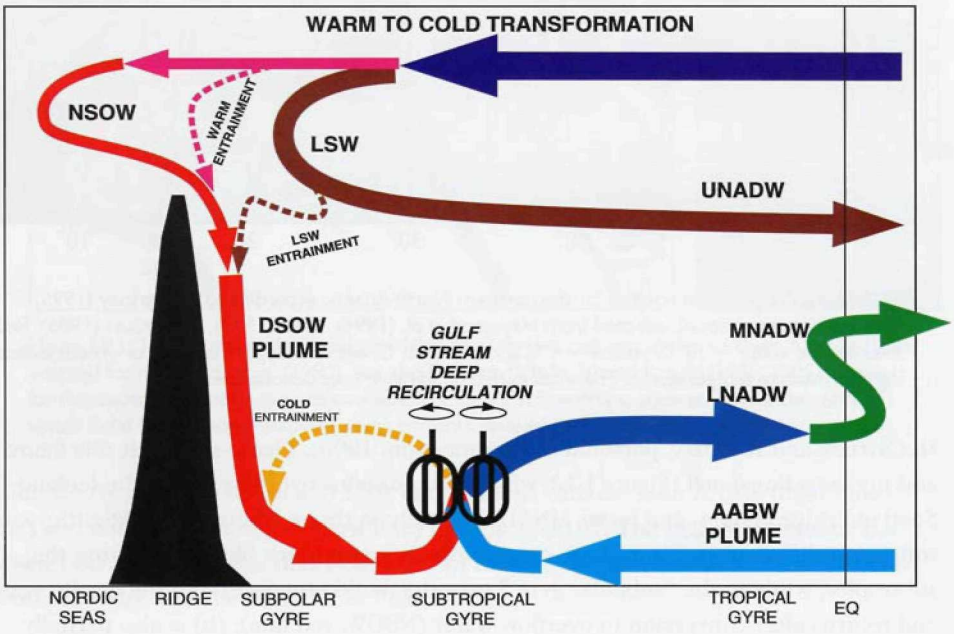

Figure I-80: A meridional schematic section of the largest-scale overturning (thermohaline) cell in the North Atlantic, including a possible mixing mechanism, according to M. McCartney and R. Curry (personal communication, 1996). See text (especially Table I-1) for water mass nomenclature.

William J. Schmitz, Jr.

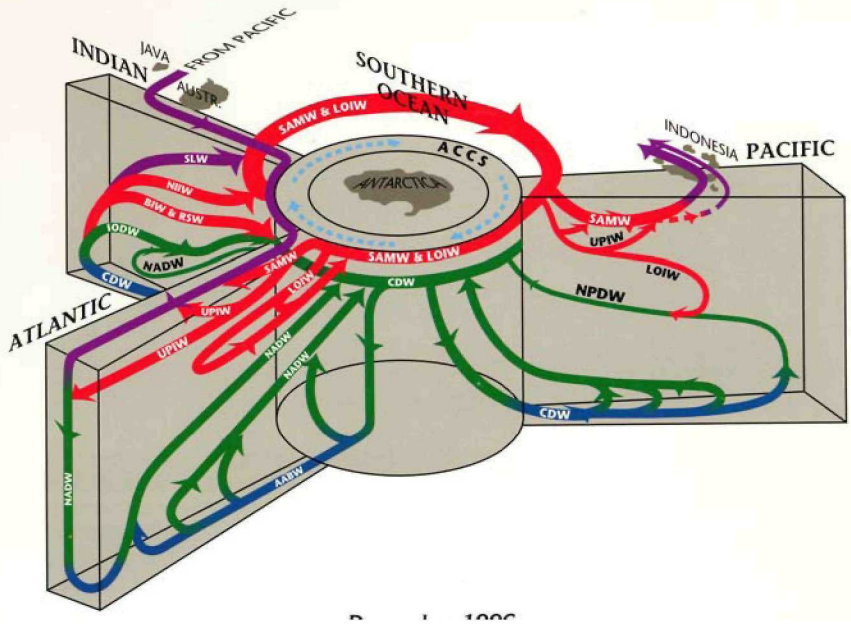

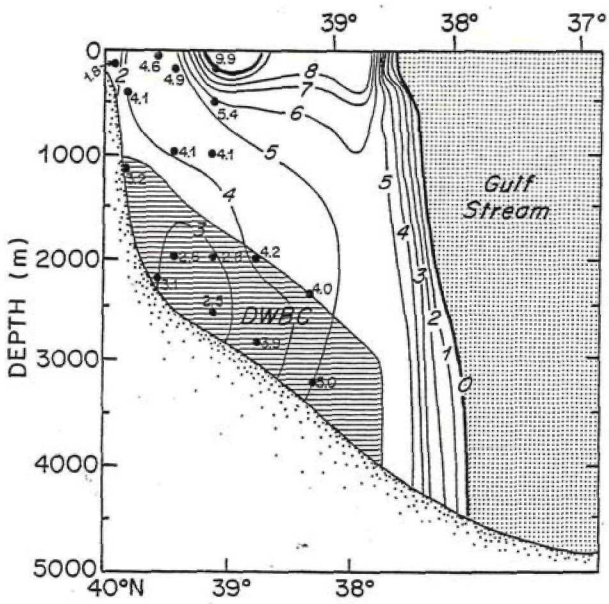

T

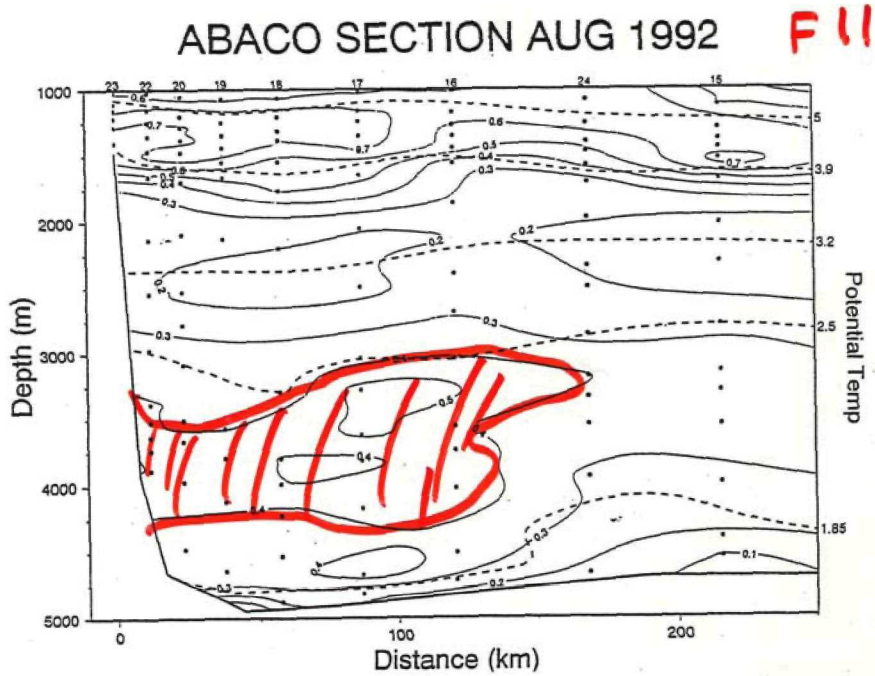

F11

Figure 3a. Section of F11 (pmol/kg) versus distance from the boundary at Abaco (26.5°N) in 1992 [Abell *et al.*, 1994].

✵ Paleo Variability

GISP and GRIP

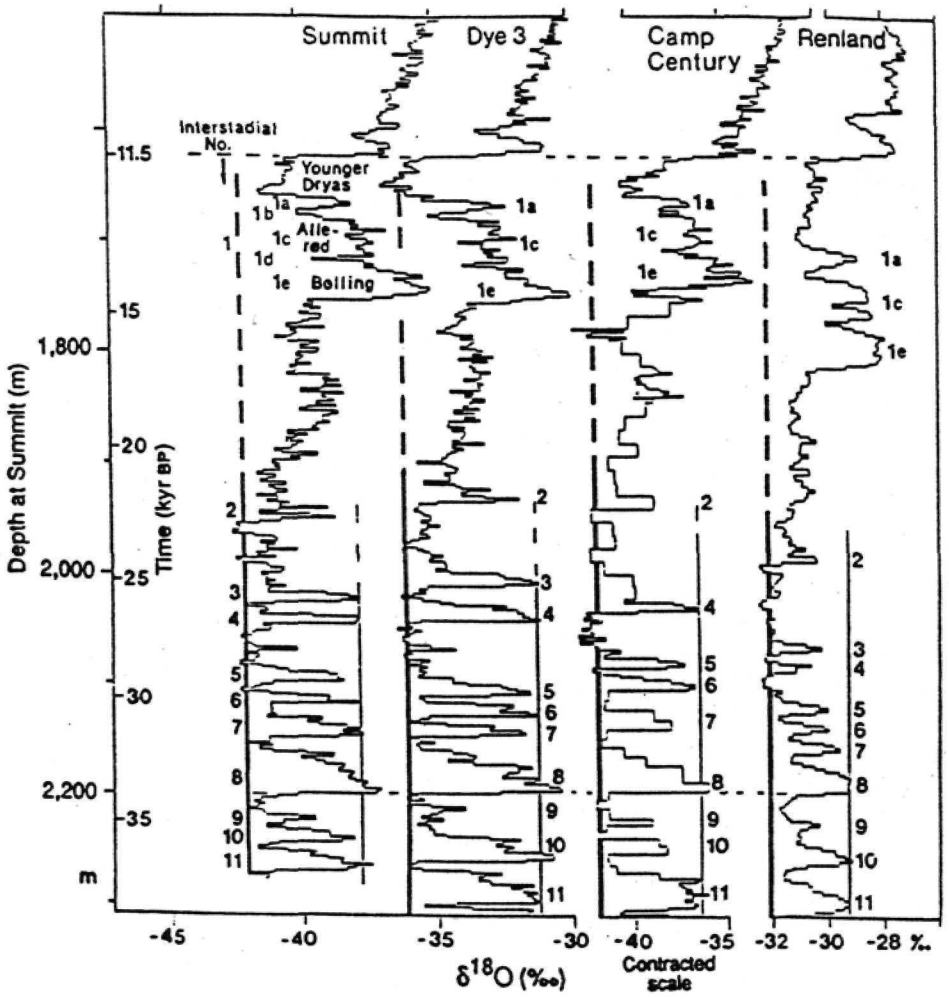

Figure 1.1: ^{18}O records from several Greenland ice cores (reproduced from Johnson, et al., 1992). Reprinted with permission from Nature (c) 1993 Macmillan Magazines Ltd.

D-O Oscillations

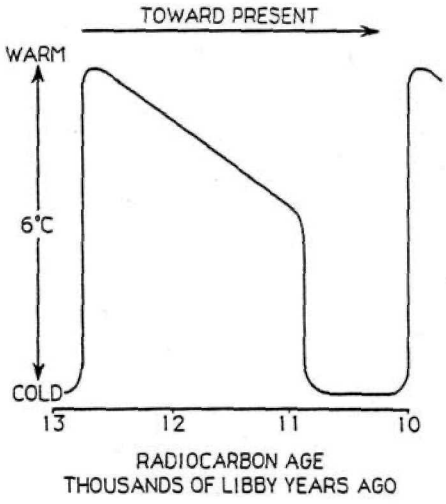

Schematic interpretation of temperature changes around the North Atlantic during the deglaciation by Broecker (redrawn from Broecker, 1991) based upon ^{18}O in ice and lake sediments, oceanic planktonic foraminifera, pollen, and beetles. See Broecker (1991) for references.

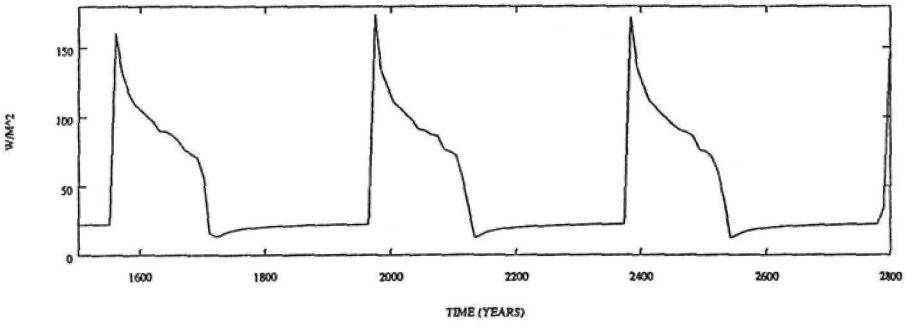

Figure 8: Upward surface heat flux (54°N to 70°N) over oscillations induced in the three dimensional model with 1.35 times the reference salt fluxes ($W \cdot m^{-2}$).

From: Winton, 1993.

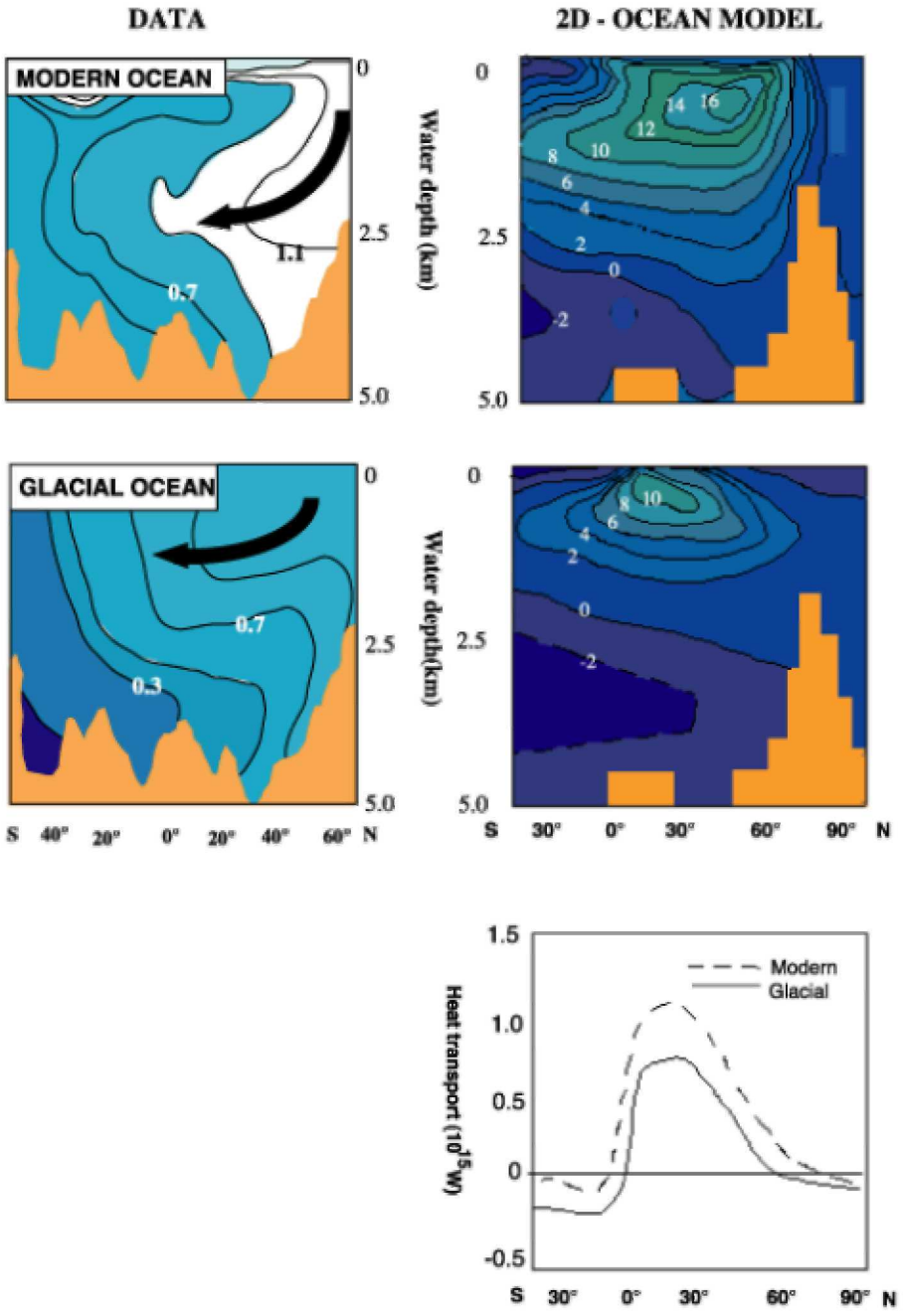

✵ Modern Variability

Changes at Depth

3. Modeling the Thermohaline Circulation

▶ The Mean Circulation

NADW ON

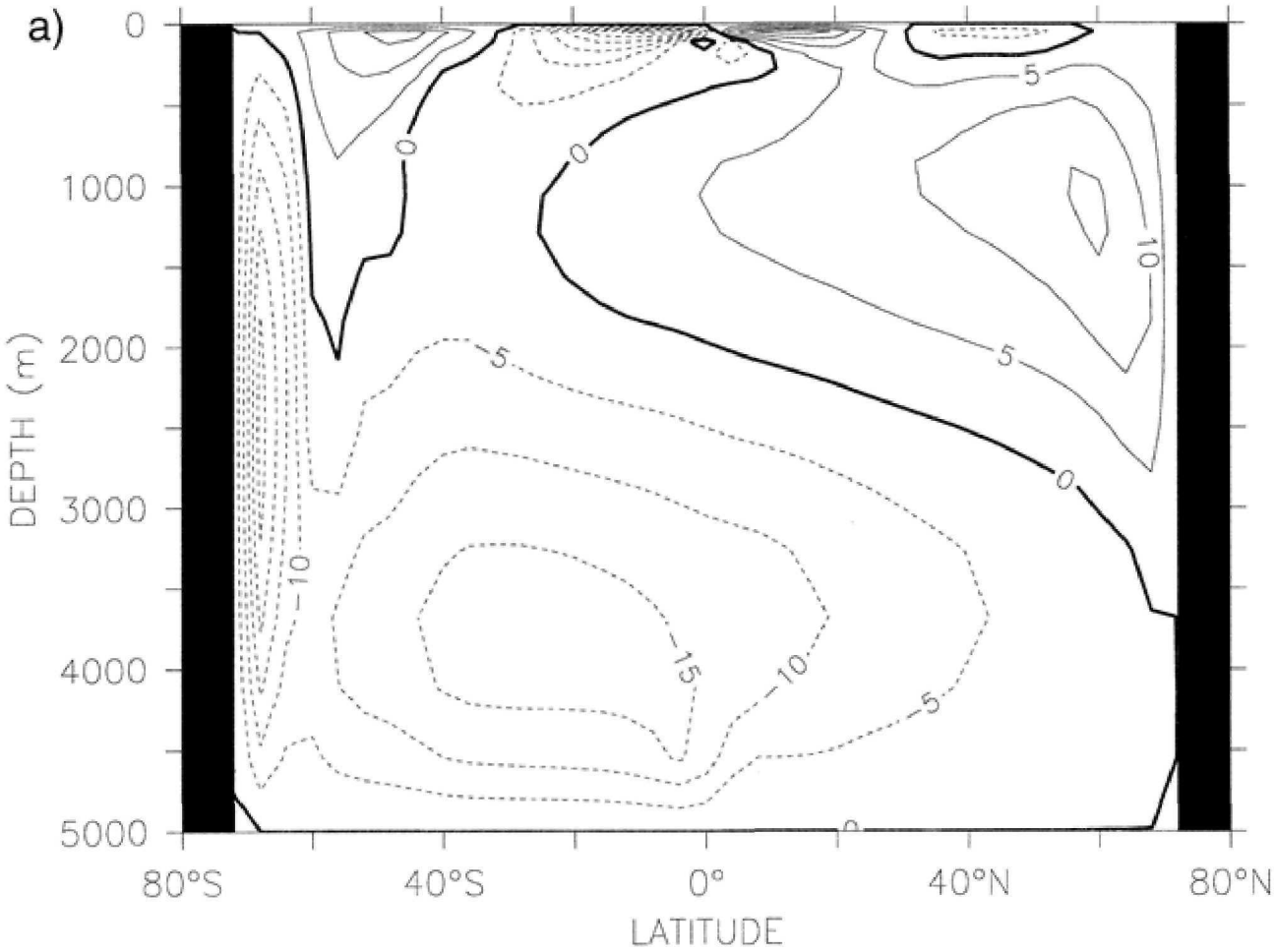

Fig. 2. Control experiment: (a) Meridional overturning streamfunction; contour interval is 5 Sv circulation.

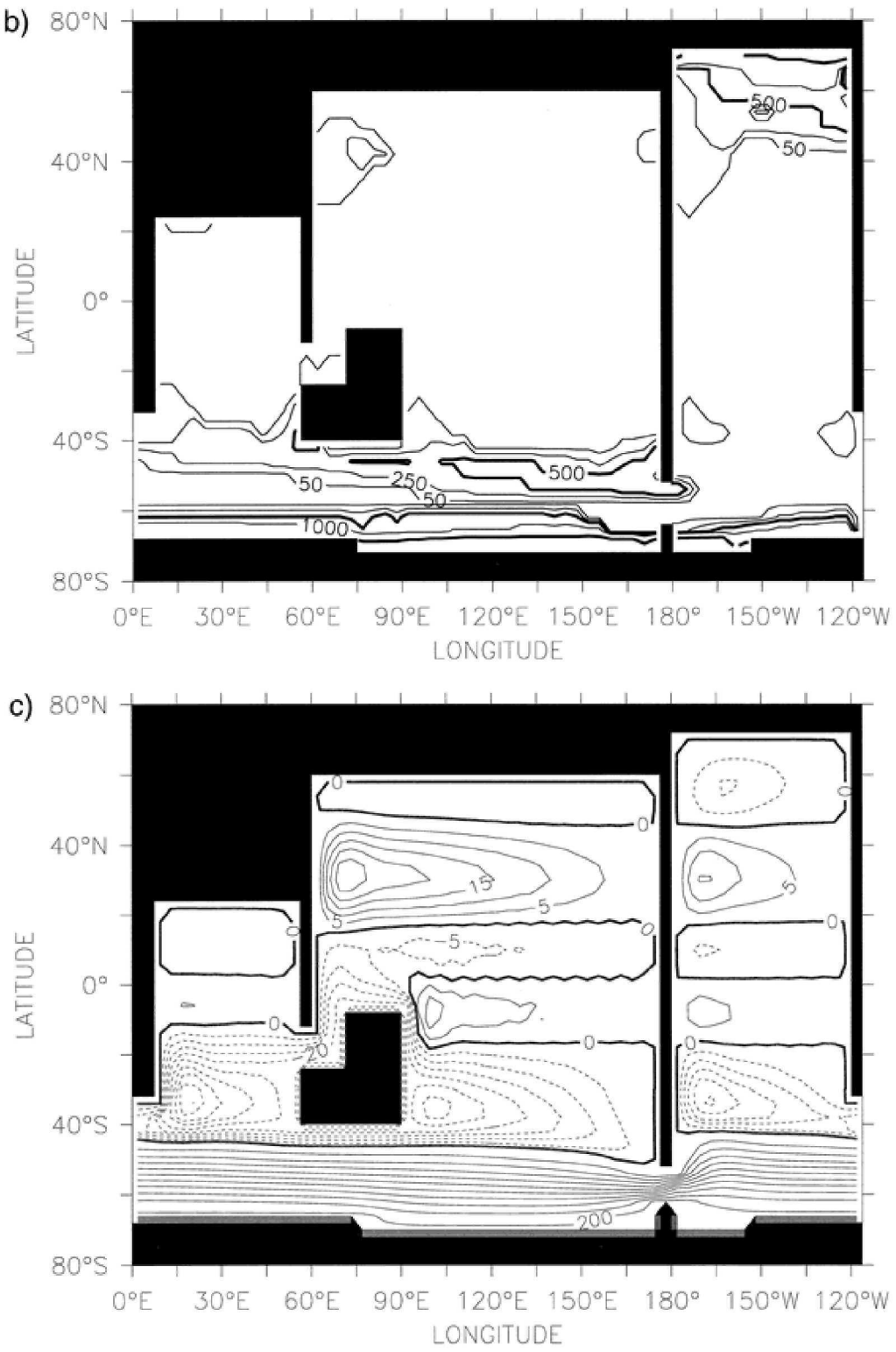

(b) Depth of convection from the surface; contours at 50, 250, 500, 1000, 2500, and 5000 m, with the 500-m and 2500-m contours darkened .. (c) Barotropic streamfunction; contour interval is 5 Sv, except in the ACC where it is 20 Sv.

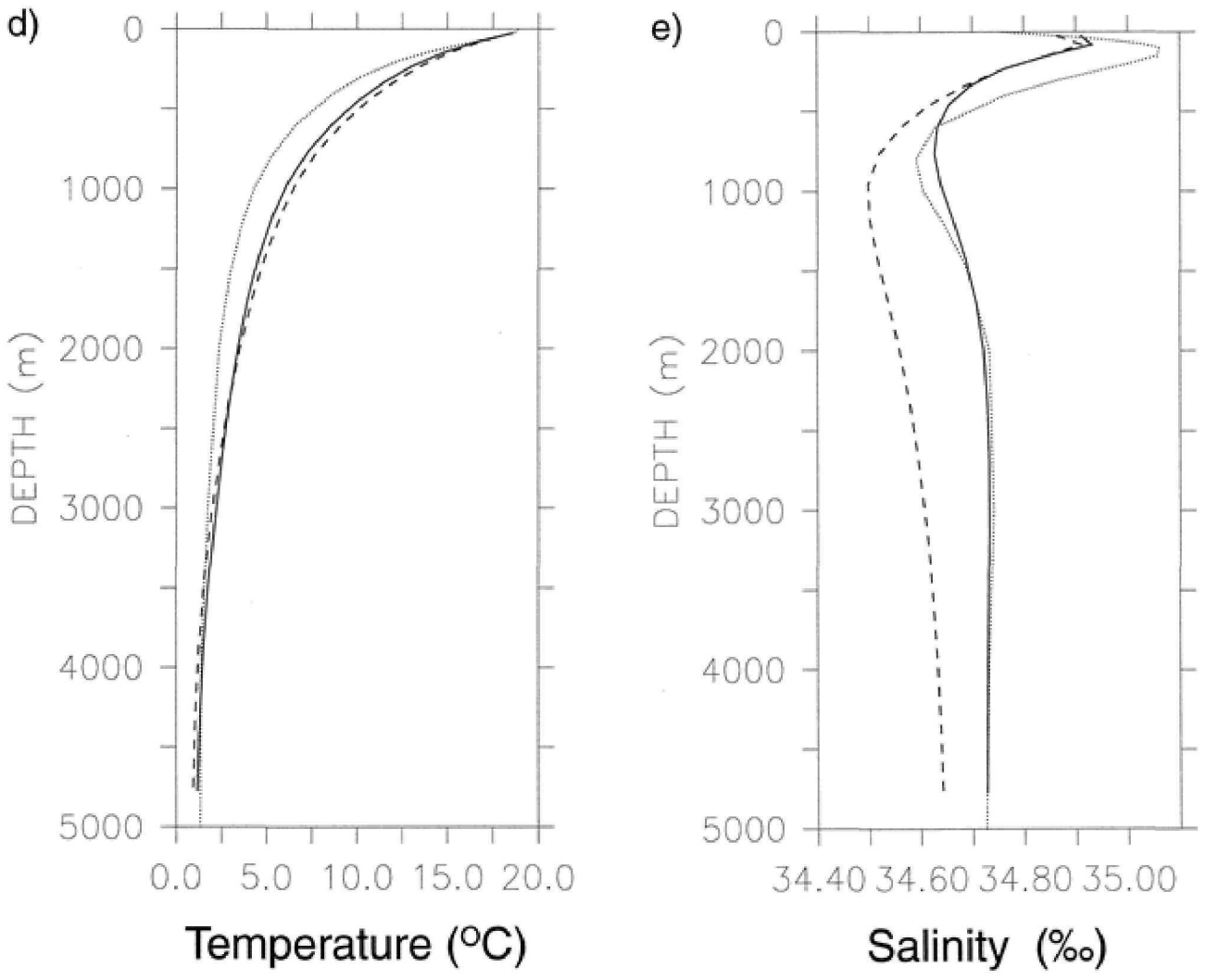

(d) Globally averaged temperature from the Control experiment (solid), No-NADW experiment (dashed), and Levitus (1982) (dotted); (e) Globally averaged salinity from the control experiment (solid), No-NADW experiment (dashed), and Levitus (1982) (dotted). Note that in (a) and (c) solid (dashed) contours denote clockwise (counterclockwise)

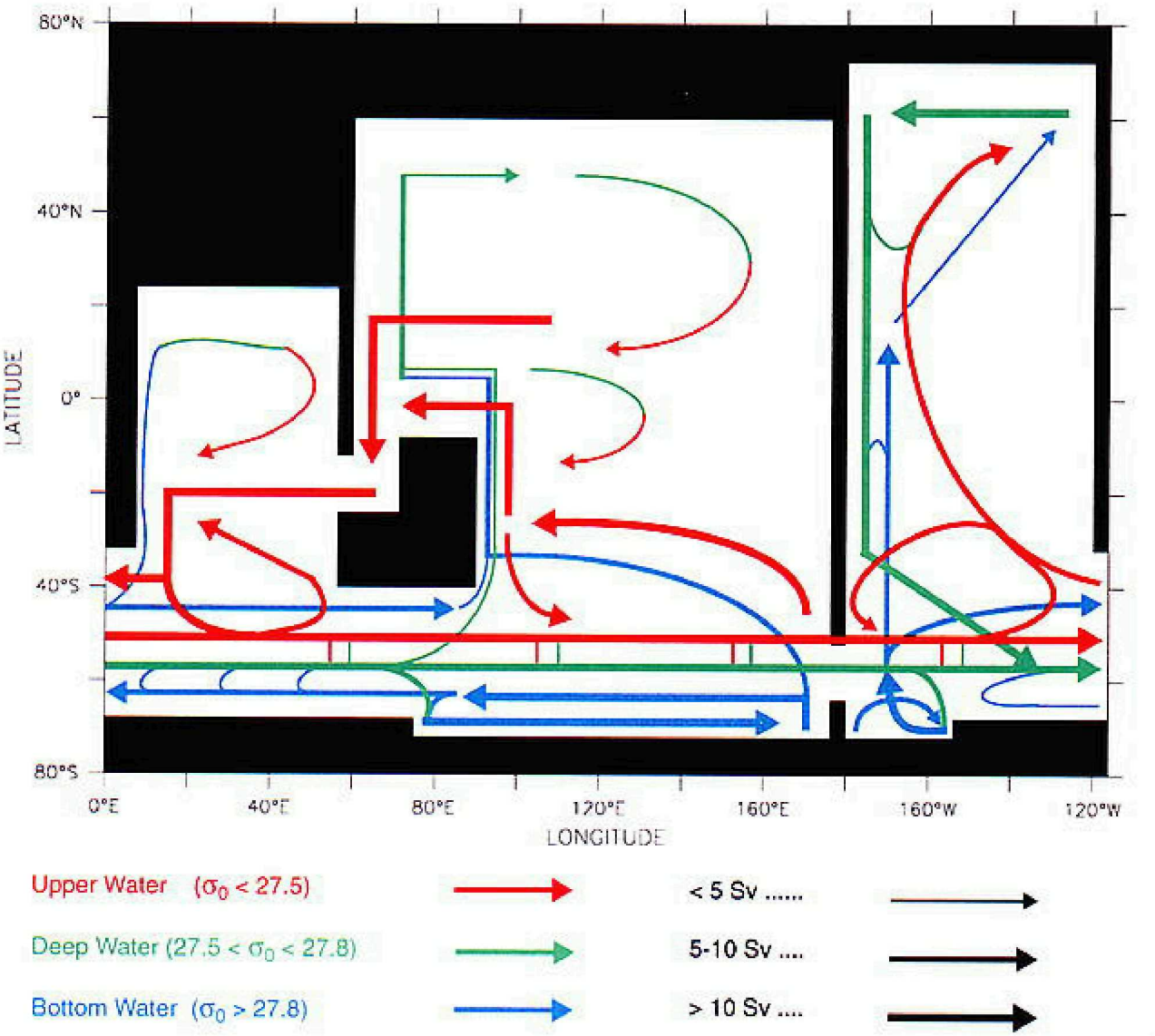

Cartoon of the model's conveyor belt circulation for the control experiment. The colors describe flows in terms of density ranges and location in the water column: red arrows indicate the combined surface and intermediate flows, green arrows indicate deep flow, and blue arrows indicate bottom flow. Note that the flow depicted by the blue arrows adjacent to Antarctica indicate an eastward surface flow of roughly the same density as the flow depicted by the westward blue arrows next to them.

NADW OFF

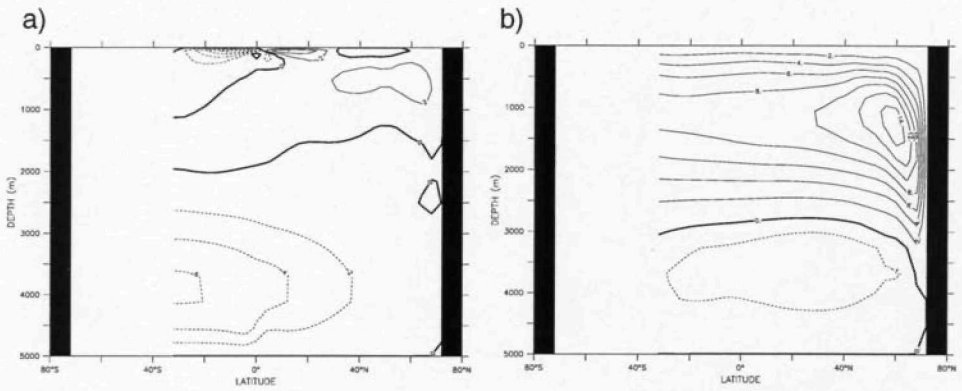

FIGURE 10 : a) No-NADW Experiment, meridional overturning streamfunction for the Atlantic Ocean only; b) Change in meridional overturning due to NADW production (Nominal Experiment - No-NADW Experiment). Contour interval in both figures is 2 Sv, with the -1 contour included in b). Solid (dashed) contours denote clockwise (counter-clockwise) circulation. (The streamfunction is undefined south of 32°S.)

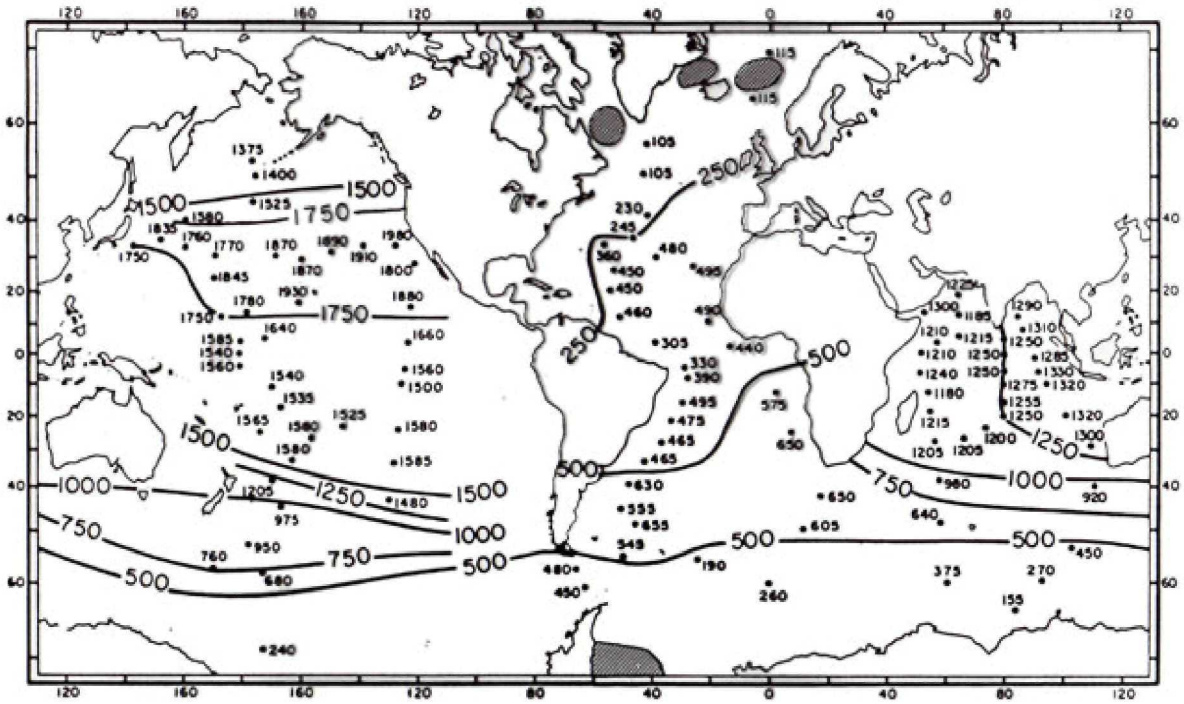

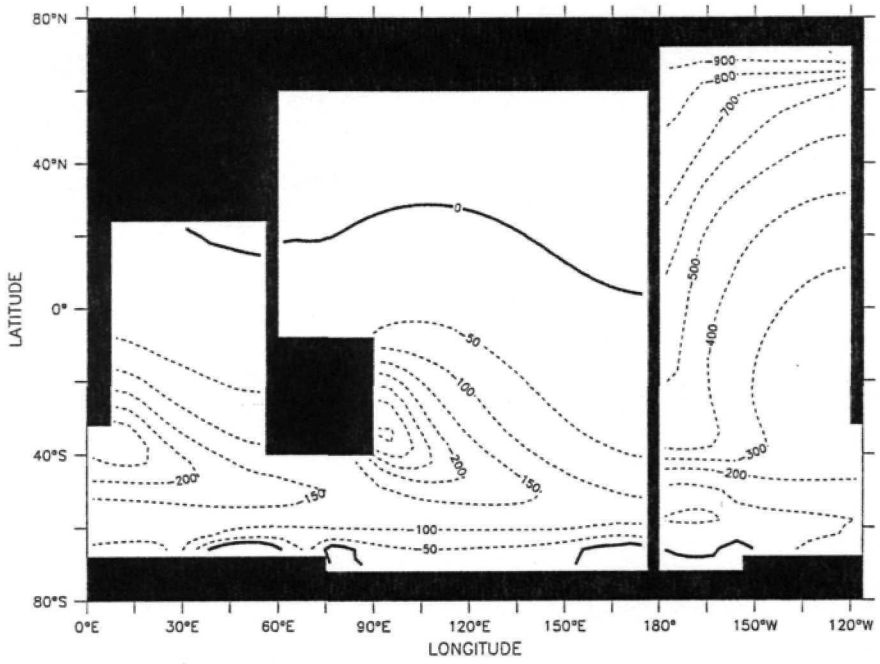

FIGURE 11 : The change in age at 2687 meters due to the production of NADW (Control Experiment - No-NADW Experiment). The contour interval is 100 years in the Atlantic sector and 50 years in the Indian and Pacific sectors.

▶Time Dependence

[The Overturning time scale due to NADW is

$$T = \frac{\text{Vol. of Ocean}}{\text{NADW Sinking (SV)}}$$

$$= \frac{1.37 \times 10^{18}\ m^3}{14 \times 10^{6}\ m^3/sec}$$

$$= 10^{11}\ sec = 3000\ yr\ ]$$

♦F. Bryan's Experiments (1987)

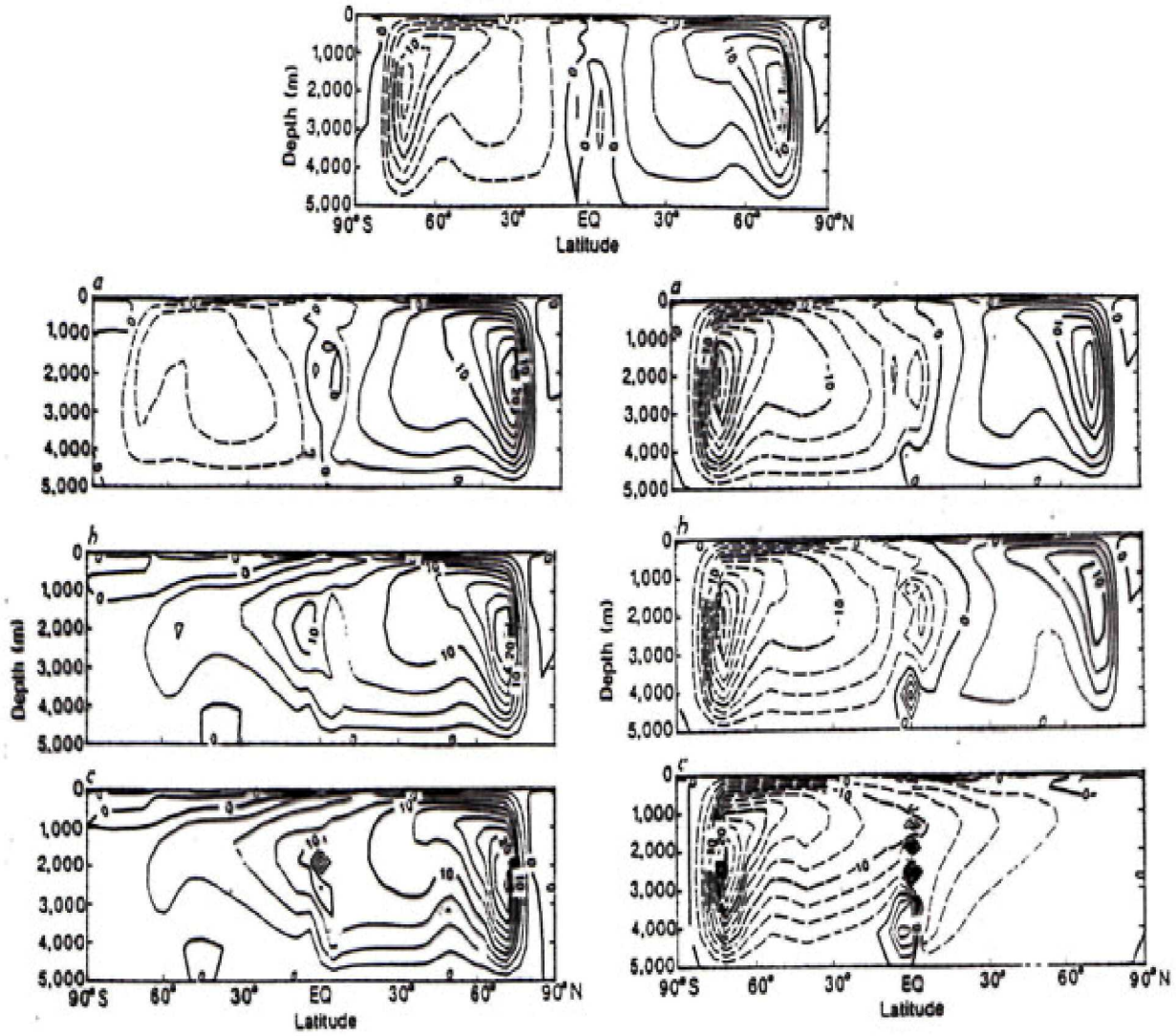

Top: Control

Left: SH Freshened a. 12yr, b. 44yr c.68 yr

Right: SH Salted a. 12yr, b. 44yr c.68 yr

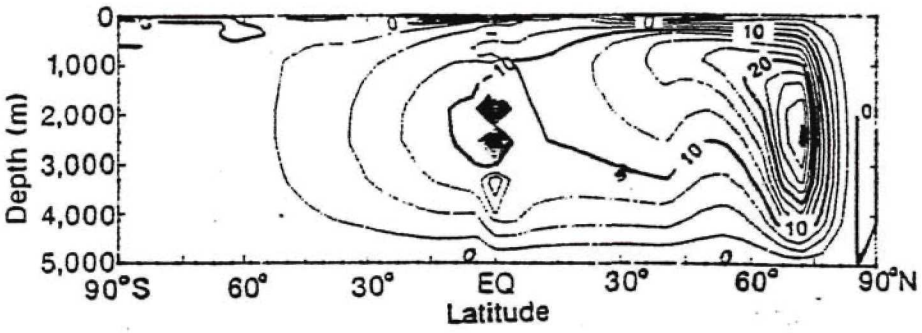

Fig. 5 Stream-function for the zonally integrated meridional overturning circulation for experiment 4 at the end of the integration. Positive values indicate a clockwise circulation; contour interval, 2.5×10^6 m^3 s^{-1}. N SALTED

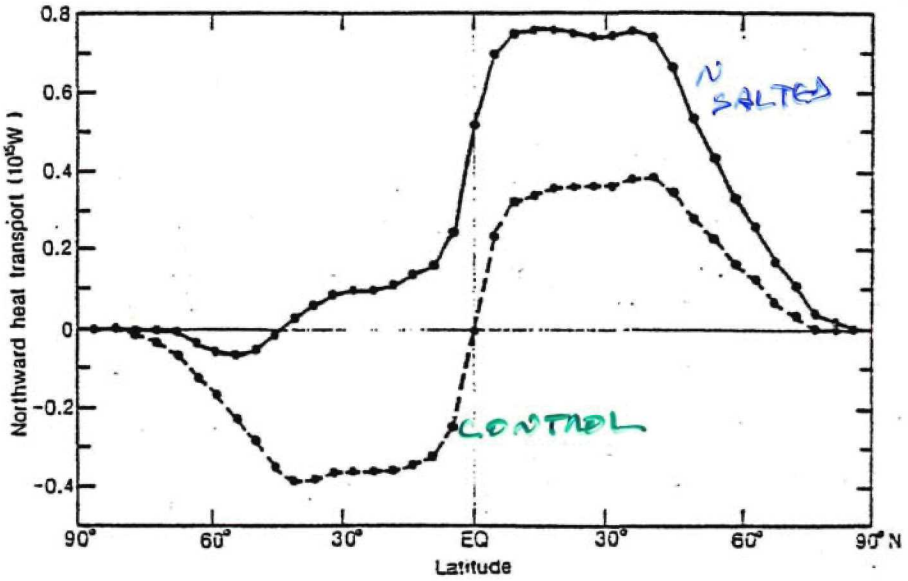

Fig. 6 Northward heat transport for experiment 4 (solid line) at the end of the integration, and for the symmetric solution obtained with newtonian-cooling-type boundary conditions on both temperature and salinity (dashed line).

♦Turning On NADW

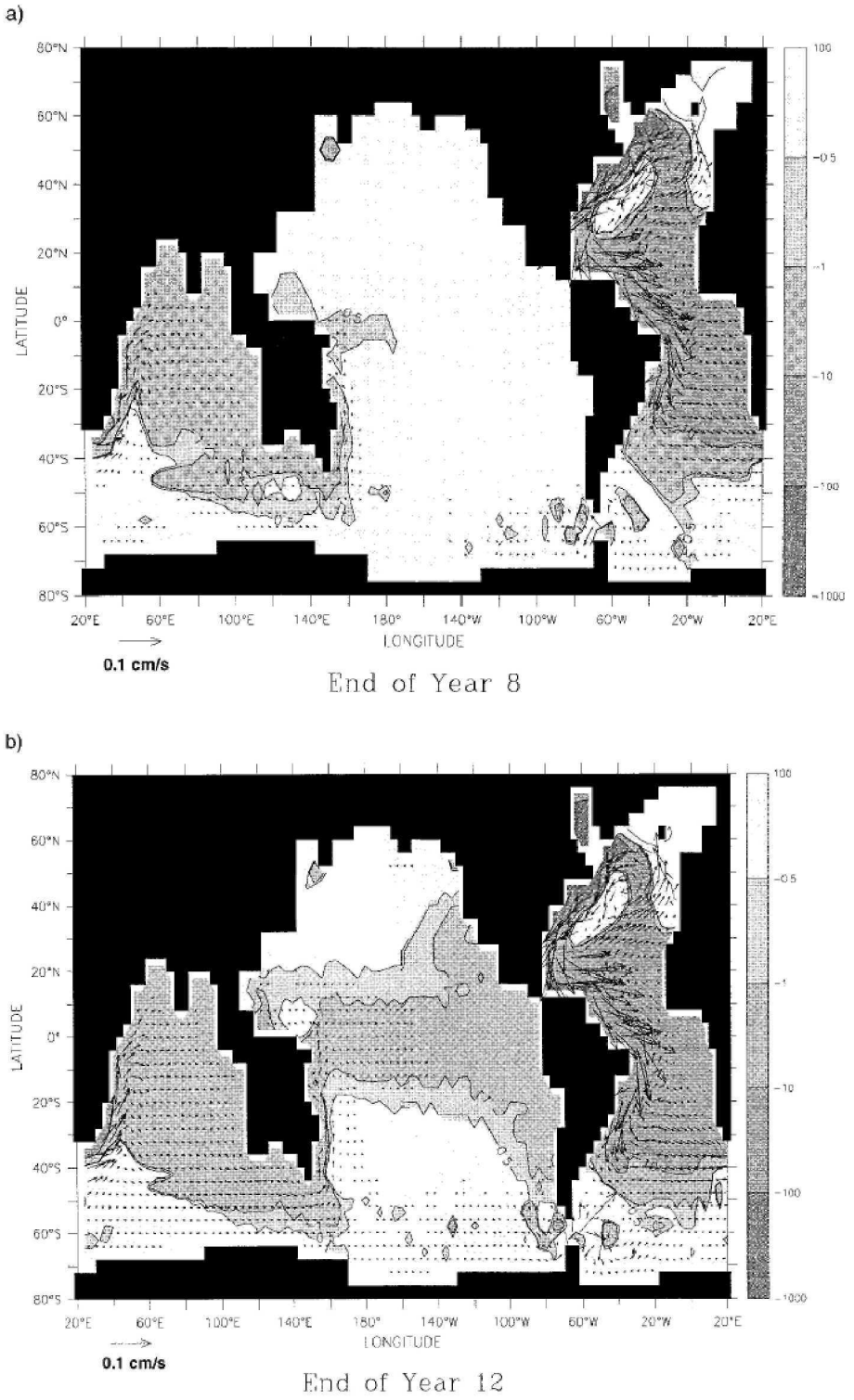

FIG. 5. The thickness anomaly between 0 and 2000 db (in mm, shaded) and the average velocity anomalies below 2000 m (vectored, vectors over 0.15 cm s^{-1}, and those north of 60°N have been omitted for clarity) after (a) year 8, (b) year 12, and (c) year 20, and (d) year 40.

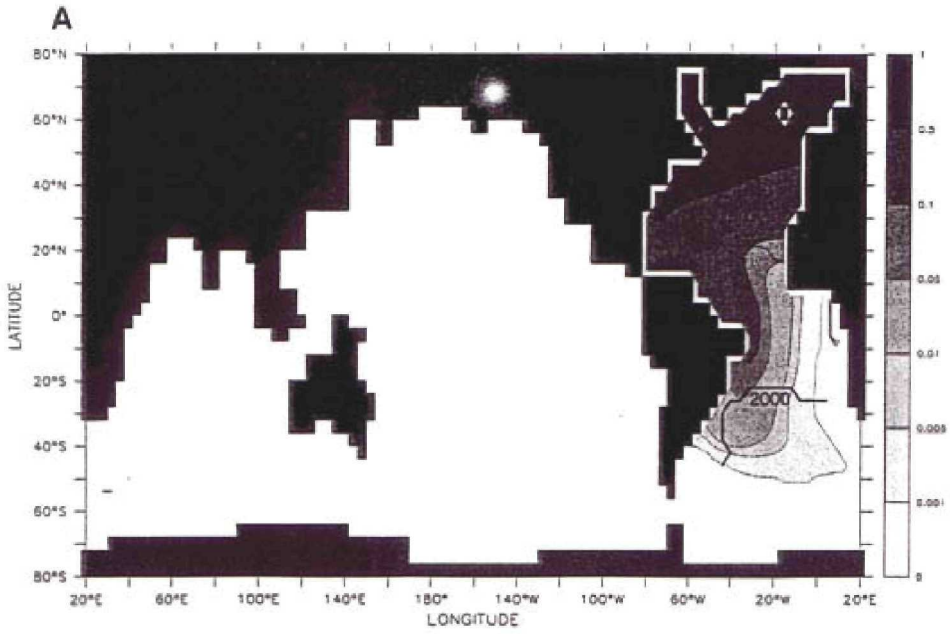

After 100 Years

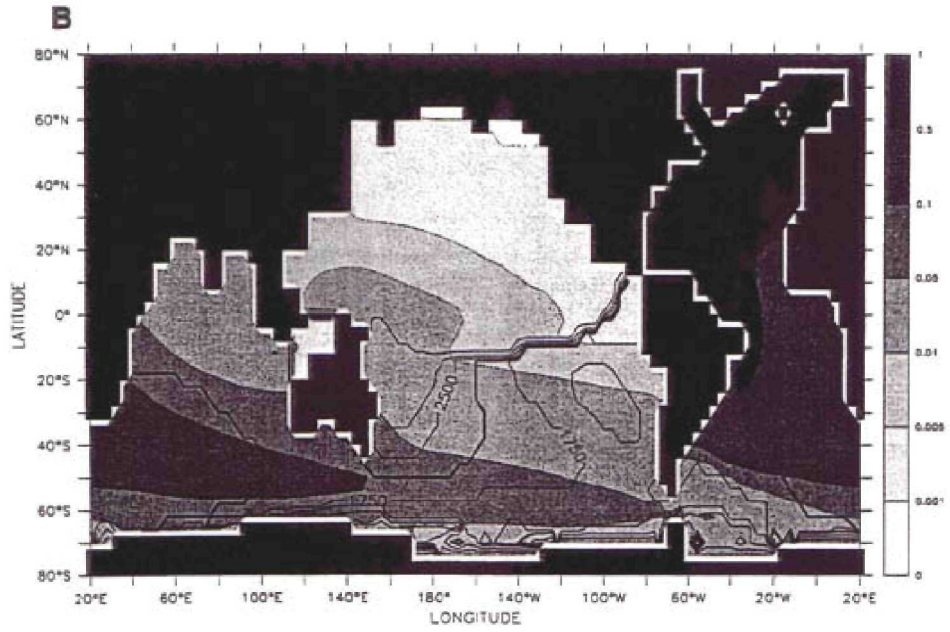

After 500 Years

4. The Connection Between the Northern and Southern Branches of the THC

a. Using Gent-McWilliams

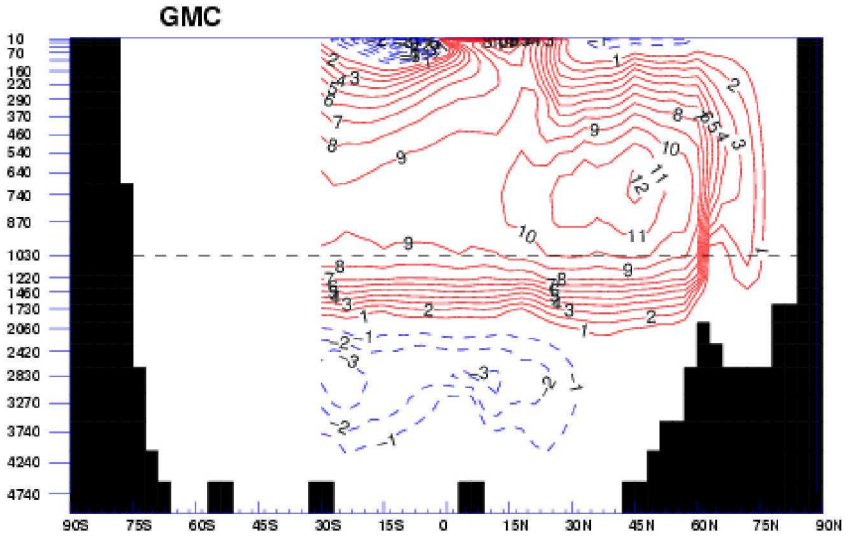

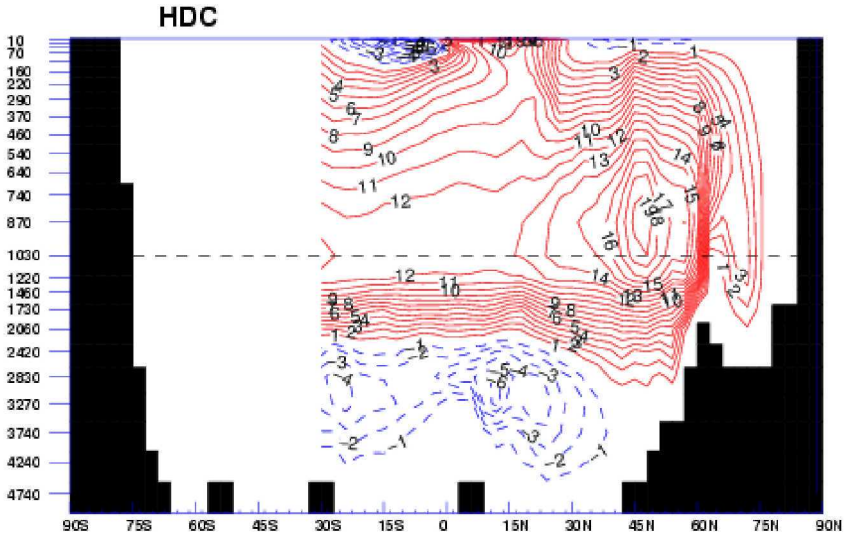

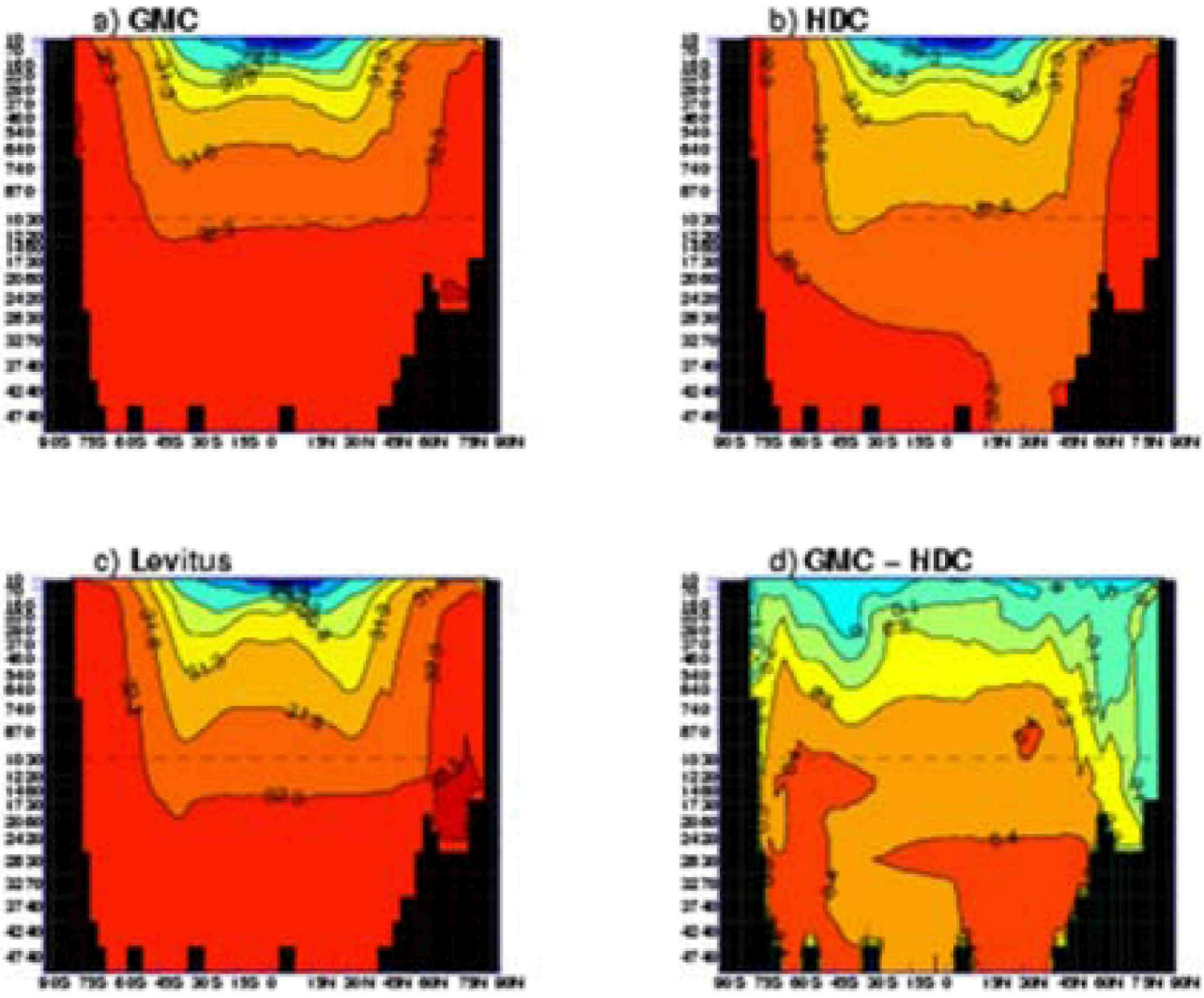

Toggweiler and McDermott and showed that increasing the winds on the ACC increases the NADW production.

5. Thermohaline Variability

✵ Multiple Equilibria

The Manabe-Stouffer Case

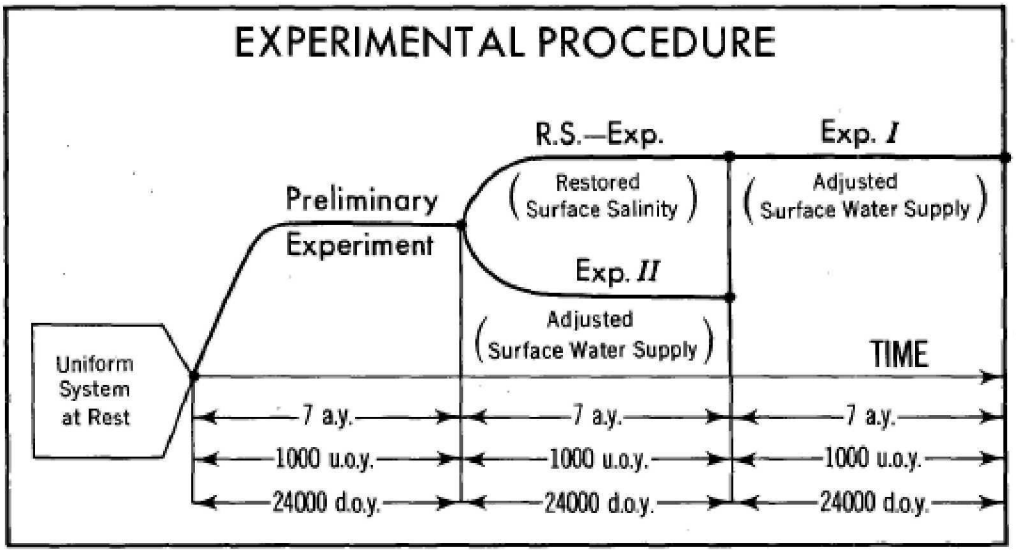

FIG. 3. Diagram which illustrates the succession of experiments conducted in the present study. For the description of the experiments, see the main text. The abbreviations a.y., u.o.y., and d.o.y. in the bottom of the figure represent atmospheric years, upper ocean years, and deep ocean years, respectively.

1. Preliminary Coupled Experiment: NO THC

2. R-S Experiment (Restore Ocean to observed Salinity): Has a THC

3. Calculate water flux needed to restore to observed.

4. Exp I has a THC, Exp II does not.

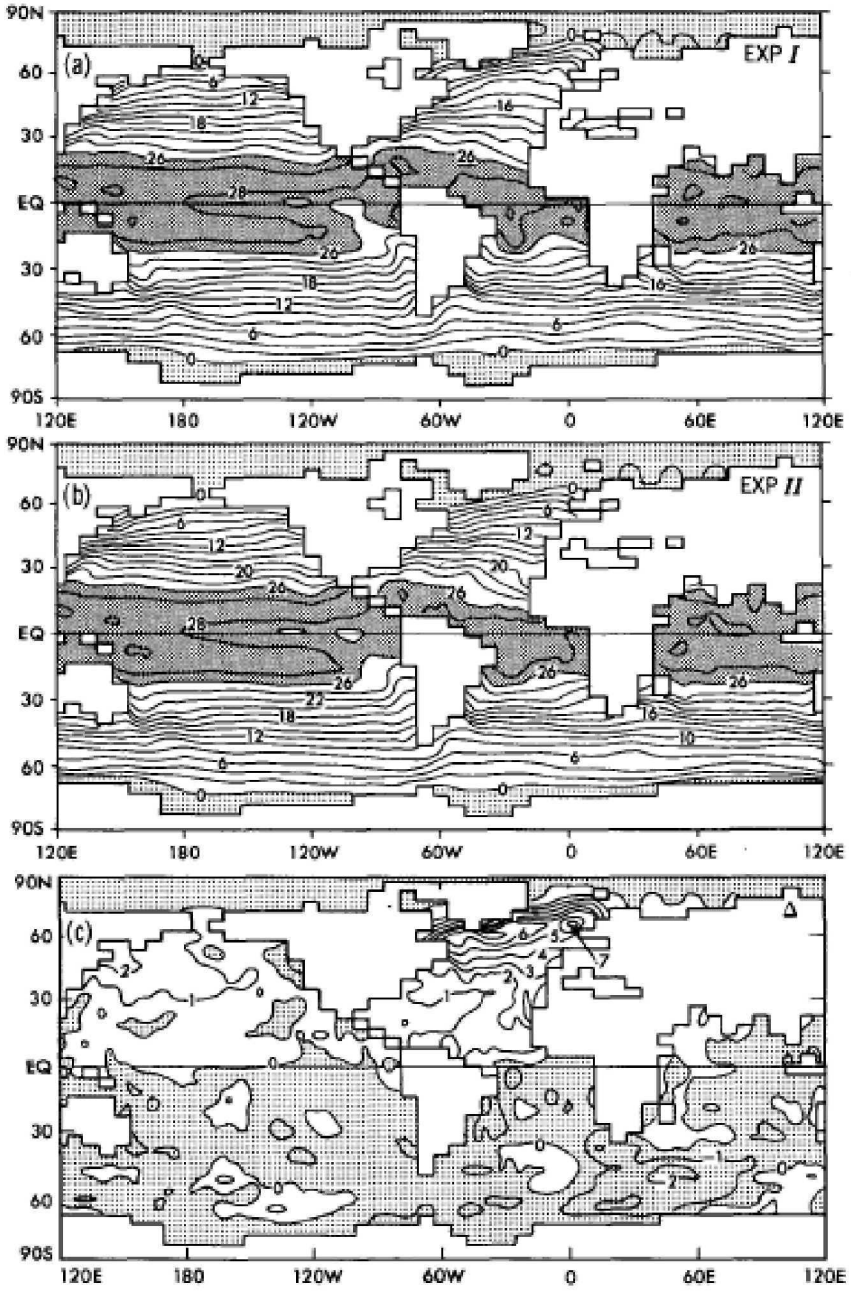

FIG. 7. (a) Sea surface temperature (degrees Celsius) from experiment I. (b) Sea surface temperature (degrees Celsius) from experiment II. (c) The difference (degrees Celsius) between the two sea surface temperatures (i.e., (a) minus (b)).

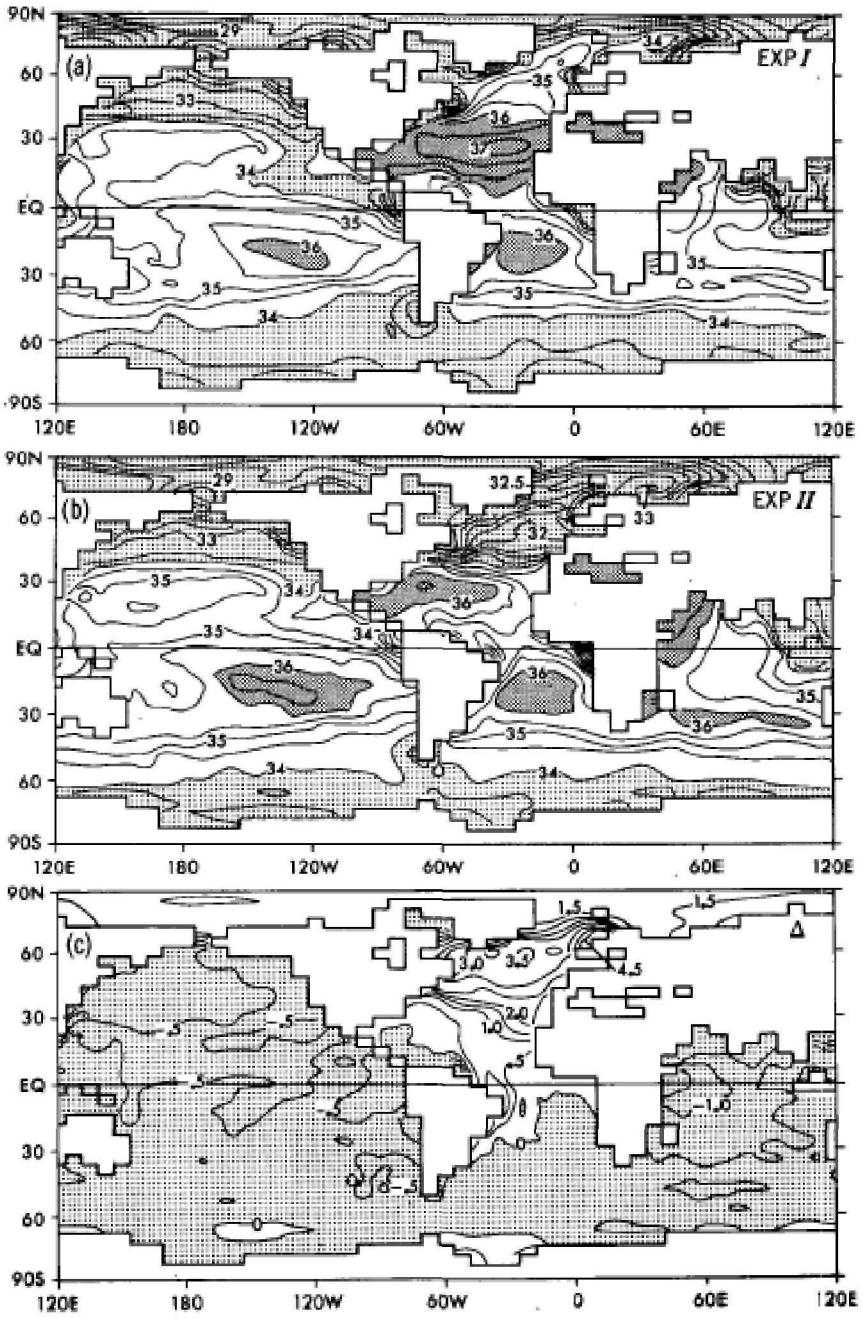

FIG. 8. (a) Sea surface salinity (ppt) from experiment I. (b) Sea surface salinity (ppt) from experiment II. (c) The difference (ppt) between the two sea surface salinity [i.e., (a) minus (b)].

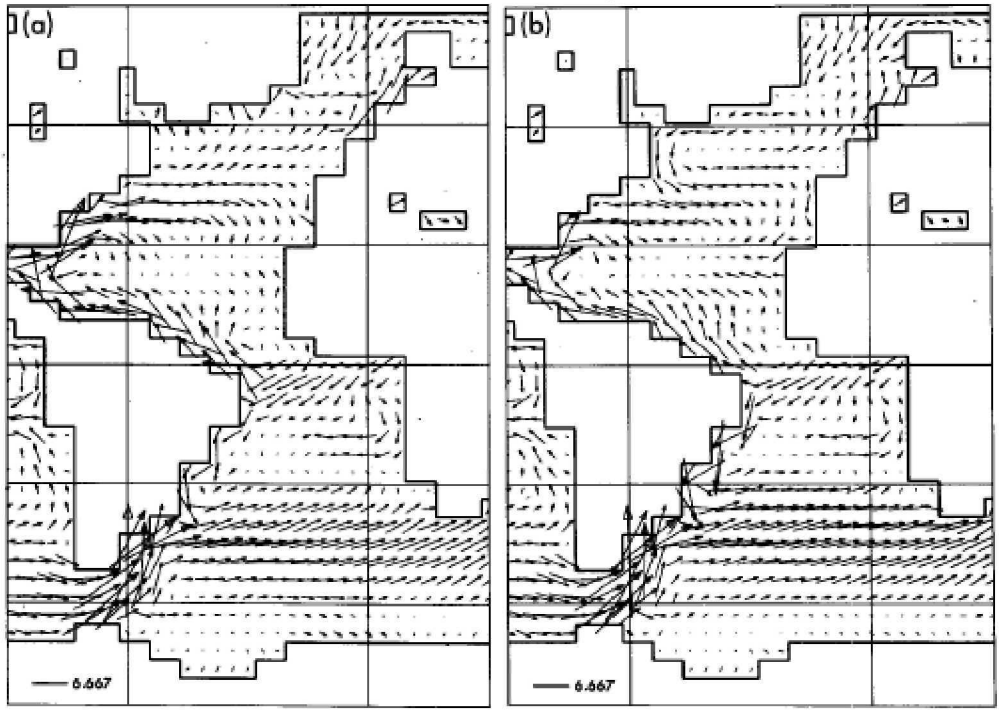

FIG. 13. Vectors of surface ocean currents in the Atlantic sector. (a) Experiment I. (b) Experiment II. See the lower left corners of each map for scaling in units of centimeters per second.

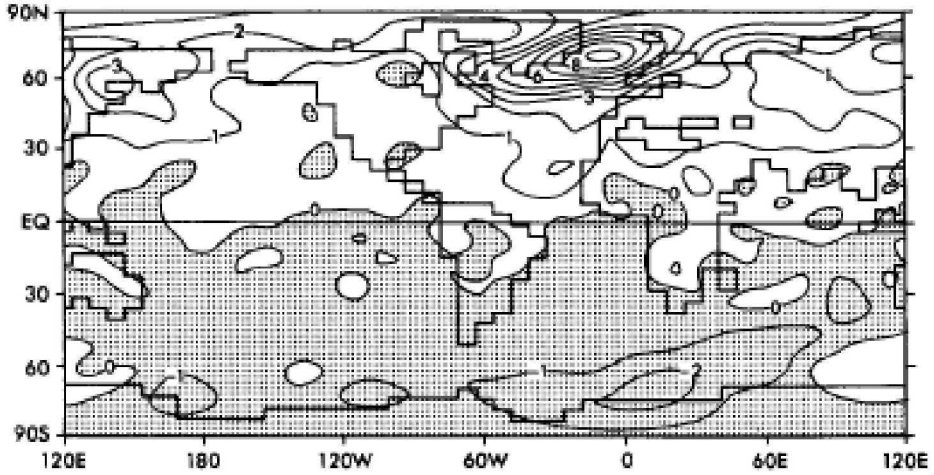

FIG. 22. Difference in surface air temperature (degrees Celsius) between experiments I and II.

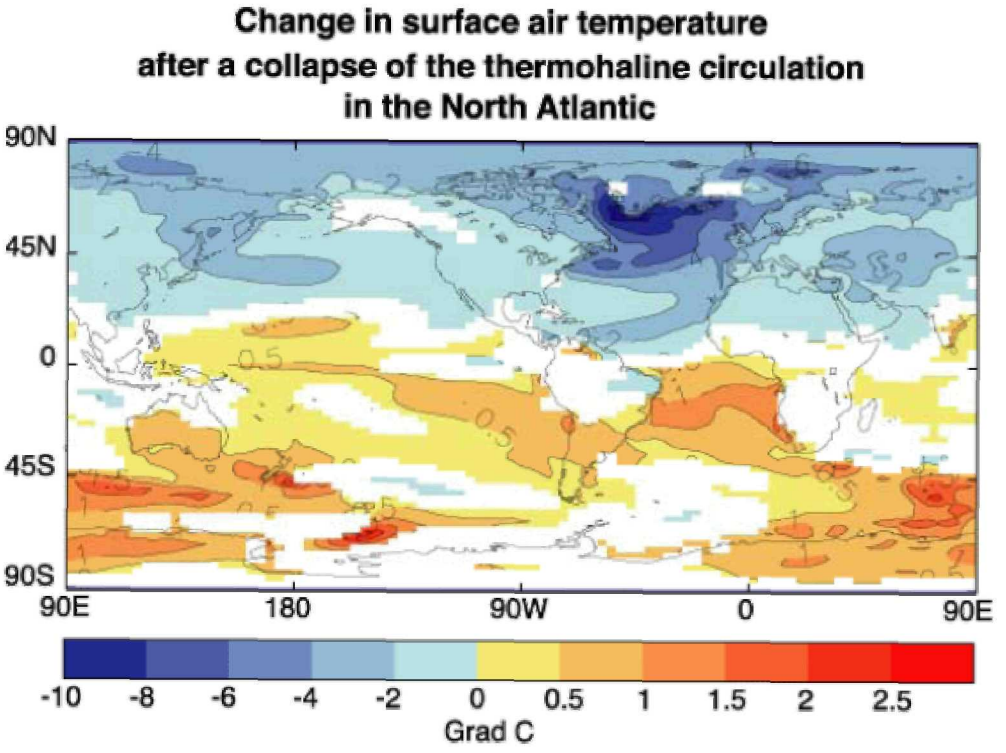

Note: the water flux adjustment is huge

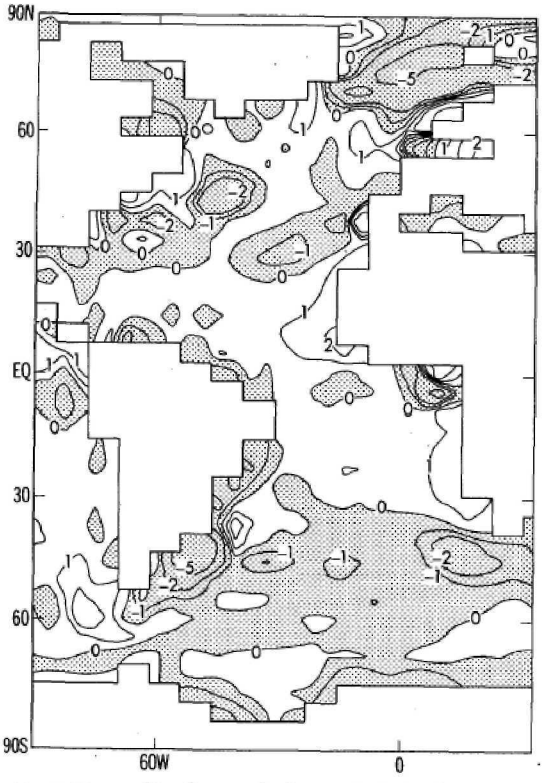

FIG. A1. The map of the adjustment of surface water flux in the Atlantic Ocean. Units are in meters per year.

❋ Stochastic Forcing

❋ Oscillatory Behavior

The basic idea:

As the Strength of Freshwater to Thermal forcing Increases, the THC becomes progressively more non-linear

Forcing

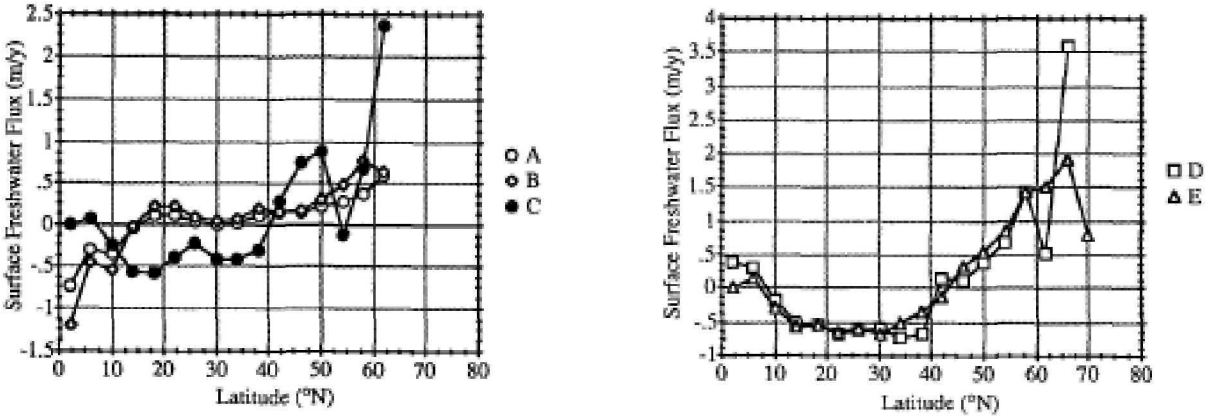

FIG. 3. (a) Zonally averaged surface freshwater gain (m yr^{-1}) as obtained from Figs. 2(a)–(c). A, B and C correspond to the restoring salinity profiles A–C that were used to obtain Figs. 2a–c. (b) As in (a) but for profiles D and E.

TABLE 2. Summary of the results of experiments for varying surface freshwater flux fields: column 1: experiment number(s); column 2: diagnosed freshwater fluxes used in mixed boundary condition integration (refer to Figs. 2 and 3). The E, $\Delta T = 3.25°C$ entry stands for $P - E$ profile "E," high-latitude SST increased by 3.25°C. Column 3: Was the spinup steady state stable on the switch to consistent mixed boundary conditions (Y or N)?; Column 4: number of steady states found under mixed boundary conditions and their stability properties; column 5: Was internal variability observed (Y or N)?; column 6: Were flushes observed (Y or N)?

Relevant expt(s).	Freshwater flux	Restoring state stable	Number of steady states found	Internal variability	Flushes
1, 2	A	Y	1 stable	N	N
3, 4	B	Y	2 stable	N	N
5–8	C	N	1 stable and 1 unstable	Y	N
9	D	N	1 unstable	Y	Y
10	E	N	1 stable and 1 unstable	Y (but very weak)	N
11	E, $\Delta T = 3.25°C$	N	1 unstable	Y	Y

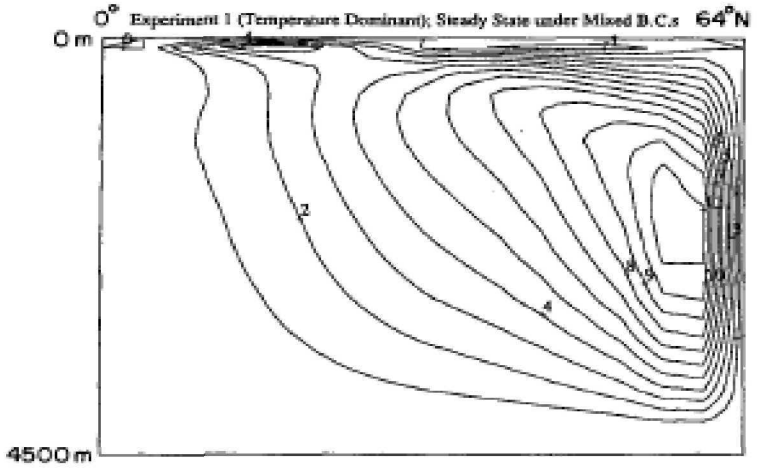

FIG. 4. Meridional overturning streamfunction [Sv (1 Sv = 10^6 m^3 s^{-1})] for the single stable equilibrium obtained in Expts. 1 and 2. Contour interval is 1 Sv.

Profile B has two stable states:

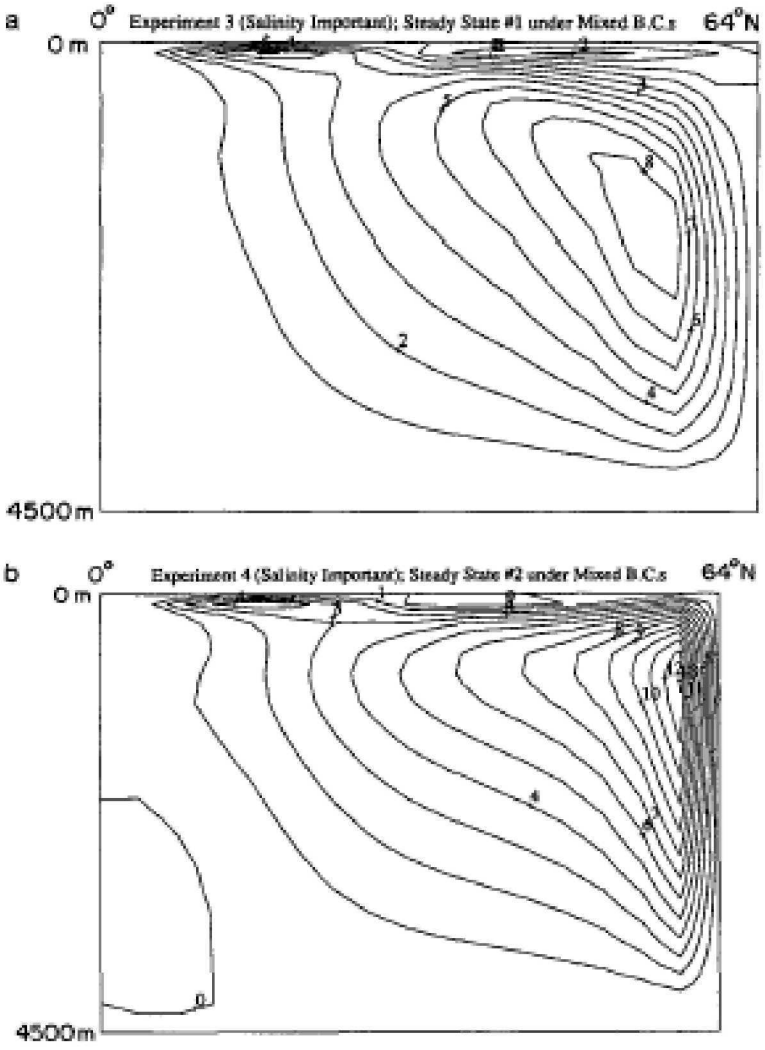

FIG. 5. Meridional overturning streamfunction (Sv) for (a) the stable steady state of Expt. 3, (b) the stable steady state of Expt. 4. Both these stable equilibria exist under the same forcing. Contour interval is 1 Sv.

Profile C has one stable, one unstable state with variability in reaching the stale state:

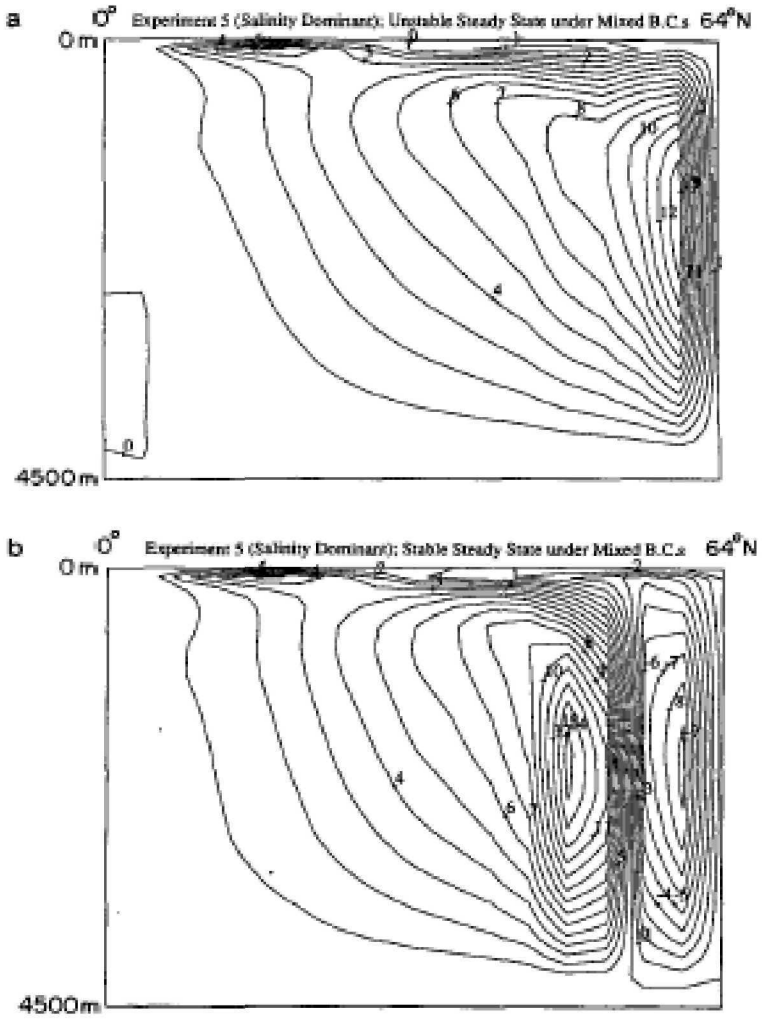

FIG. 6. Meridional overturning streamfunction (Sv) for (a) the unstable steady state of Expt. 5 under mixed boundary conditions, (b) the stable steady state of Expt. 5 under the same mixed boundary conditions. Contour interval is 1 Sv.

with considerable variability in reaching the stable state:

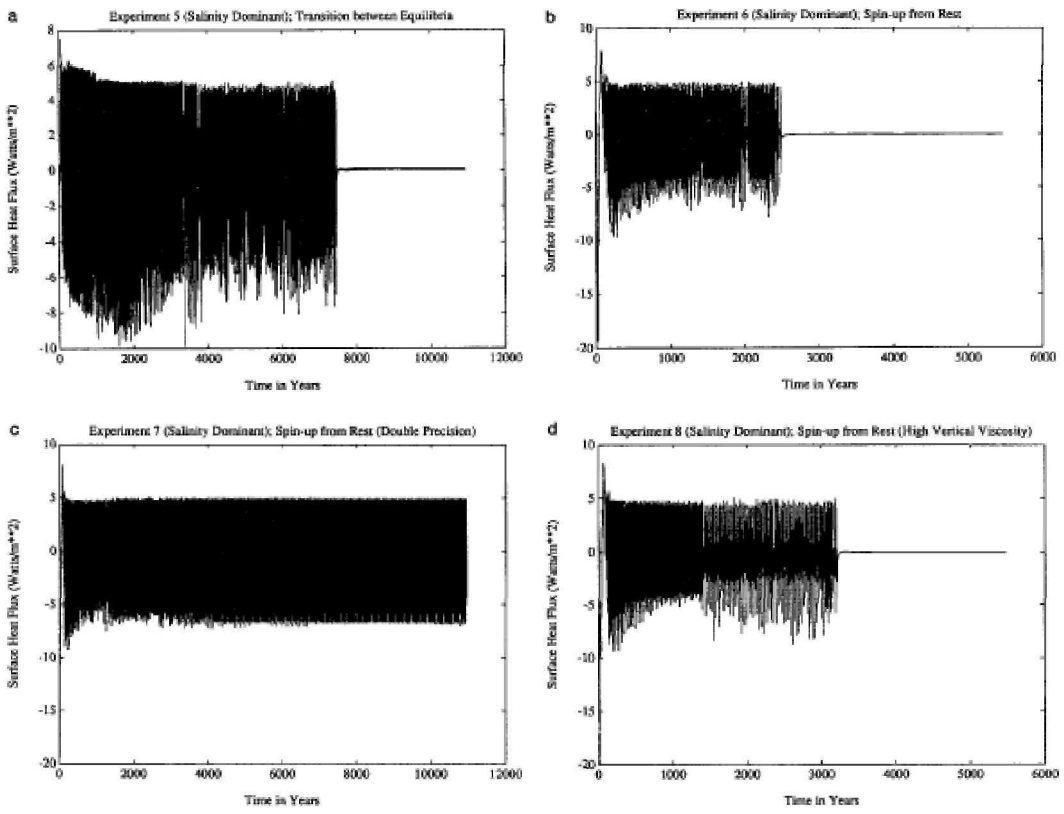

FIG. 7. Net basin-averaged surface heat gain (W m^{-2}) for the four experiments using the freshwater flux profile C (see Figs. 2c and 3a). (a) Experiment 5 (transition from the unstable equilibrium of Fig. 6a to the stable equilibrium of Fig. 6b). (b) Experiment 6 (spinup from a homogeneous resting ocean). (c) Experiment 7 [as in (b) but using double precision]. (d) Experiment 8 [as in (c) but using a higher vertical viscosity A_{MV} = 100 cm^2 s^{-1}].

Profile D gives suppression of THC punctuated by "flushes":

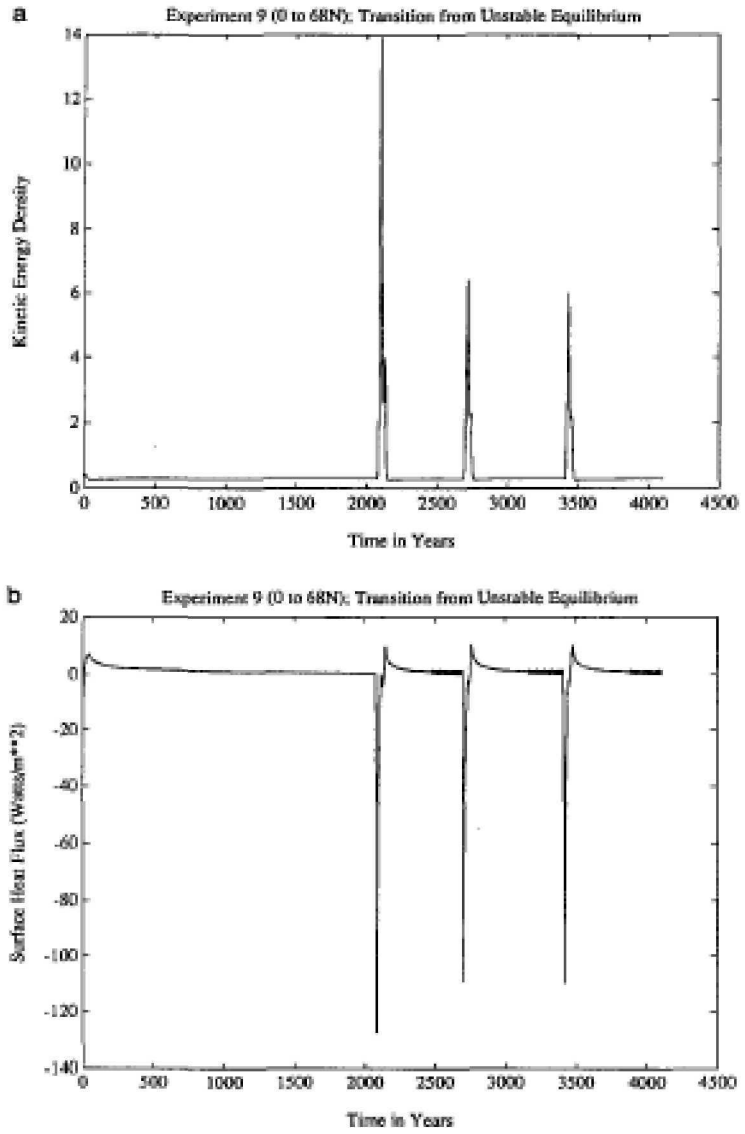

FIG. 10. (a) Kinetic energy density (10^{-1} kg m^{-1} s^{-2}) over the entire integration for experiment 9 (freshwater flux profile D in Figs. 2d and 3b). (b) As in (a) but for the net surface heat uptake (W m^{-2}) averaged over the entire basin.

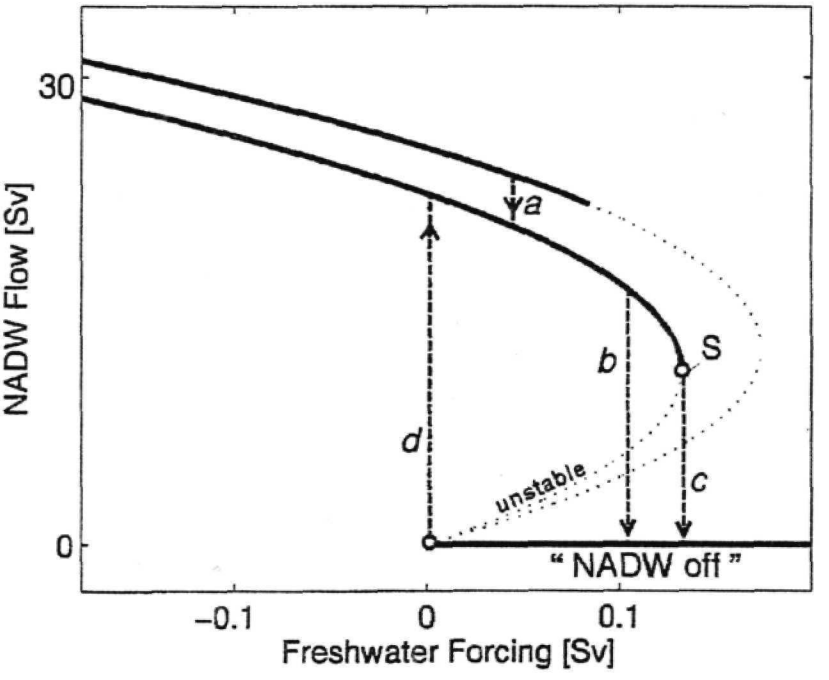

Fig. 15.3 Schematic bifurcation diagram for North Atlantic Deep Water (NADW) flow, as derived from GCM results and theoretical models. Solid lines show stable equilibrium states; unstable states are dotted. The upper two solid lines correspond to equilibria with different NADW formation sites, the bottom one to an equilibrium without NADW formation. The uppermost stable branch is not drawn out to its saddle-node bifurcation, indicating that it becomes convectively unstable before reaching the advective stability limit. Examples of the four basic transition mechanisms are shown by dashed lines: (**a**) local convective instability, a rapid shutdown or startup of a convection site, (**b**) polar halocline catastrophe, a total rapid shutdown of North Atlantic convection, (**c**) advective spindown, a slow spindown process triggered when the large-scale freshwater forcing exceeds the critical value at Stommel's saddle-node bifurcation S while convection initially continues, (**d**) startup of convection in the North Atlantic from a "NADW off" state. The convective transitions a, b, d can be triggered either when a gradual forcing change pushes the system to the end of a stable branch or by a brief but sufficiently strong anomaly in the forcing.

5. Thermohaline Circulation Under Global Warming

Manabe and Stouffer:

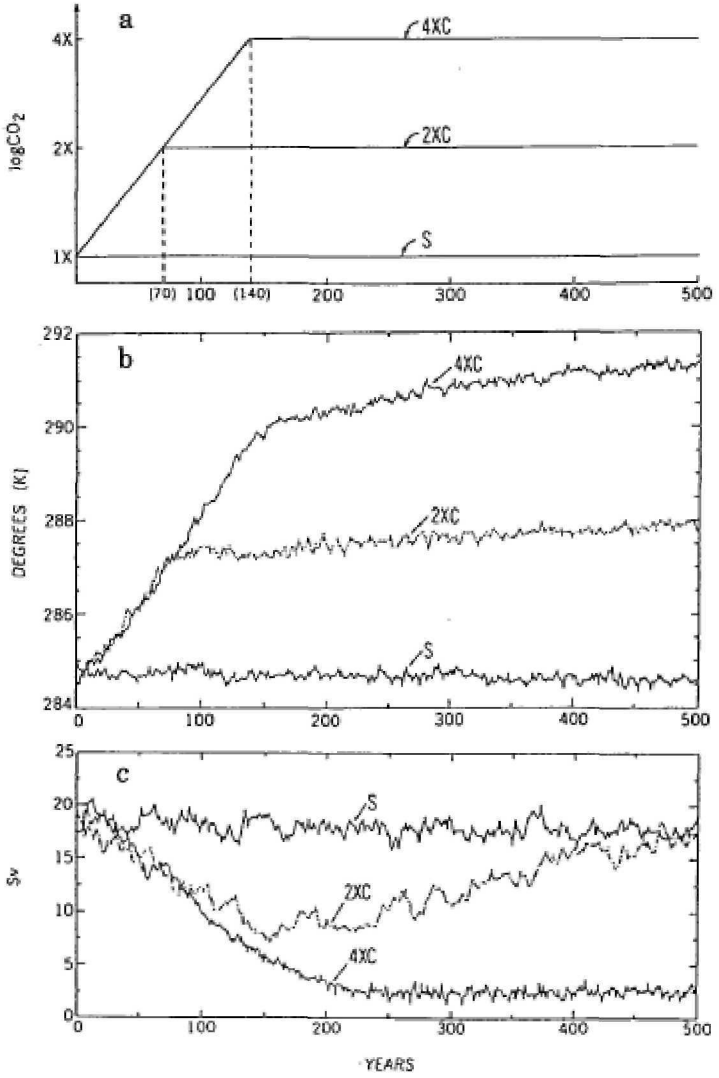

Fig. 12. Temporal variations of: (a) logarithm of atmospheric CO_2 concentration; (b) global mean surface air temperature (K); (c) the intensity of the THC in the north Atlantic; obtained from 4 × C, 2 × C and S (from MS94). Here, the intensity of the THC is defined as the maximum value (Sv) of the streamfunction representing the meridional overturning in the North Atlantic Ocean.

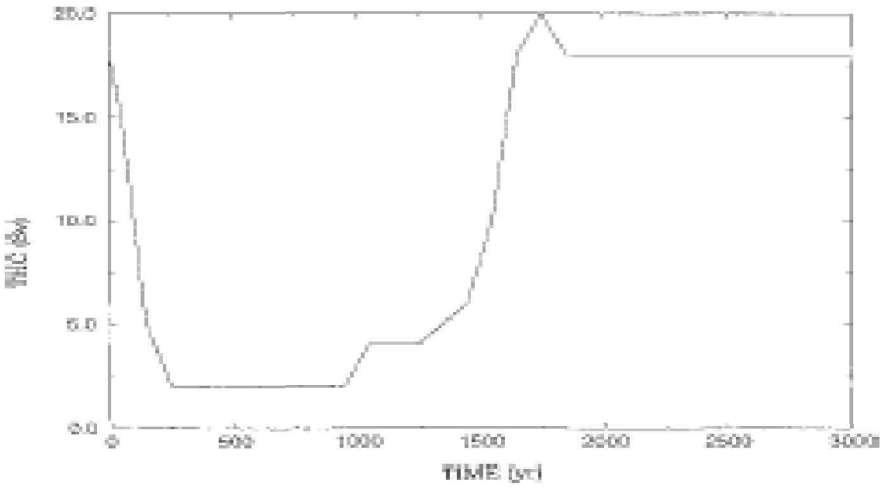

Fig. 15. Time series of the 100-year mean intensity of the THC (Sv) obtained from the 4 × C integration of the coupled model over the period of 3000 years (from MS94). Here, the intensity of the THC is defined as the maximum value of streamfunction representing the meridional overturning in the North Atlantic Ocean.

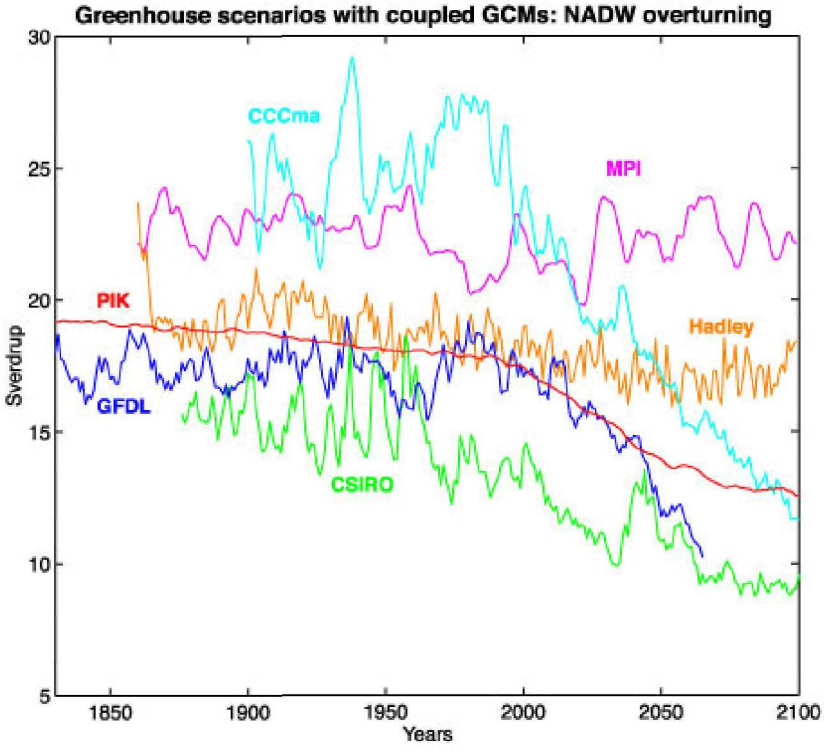

PIK: CLIMBER2 (Potsdam)

GFDL: R15 (Princeton)

CSIRO: GM version (Melbourne)

CCCma: GCM2/MOM1.1 (Victoria)

MPI: ECHAM4/OPYC (Hamburg)

Hadley: HADCM2 (Bracknell)

(Compiled by Stefan Rahmstorf)

REFERENCES

Bryan, F., 1986: High latitude salinity effects and inter-hemispheric thermohaline circulations. *Nature*, **323**, 301-304.

Goodman, P. J., 2001: Thermohaline adjustment and advection in an OGCM. *J Phys. Oceanogr.*, **31**, 1477-1497.

Goodman, P. J., 1998: The role of North Atlantic Deep Water formation in an OGCM's ventilation and thermohaline circulation. *J. Phys. Oceanogr.,* **28**, 1759–1785

Huang, R. X., M. A. Cane, N. Naik, and P. J. Goodman, 2000: Global adjustment of the thermocline in response to deep water formation, *Geophys. Res. Lett.,* ,**27**, 756-762.

Kamenkovich, I.V., and E.S. Sarachik, 2003: Mechanisms controlling the sensitivity of the Atlantic thermohaline circulation to the parameterization of eddy transports in an ocean GCM. *J. Phys. Oceanogr*. Submitted.

Manabe S., and R.J. Stouffer, 1988: Two stable equilibria of a coupled ocean-atmosphere model. *J. Climate:* 1, 841–866.

Manabe S., and R.J. Stouffer, 1999: The role of thermohaline circulation in climate. *Tellus*, 51, 91-109.

McDermott, D. A., 1996: The Regulation of Northern Overturning by Southern Hemisphere Winds. *J.Phys. Oceanog.* **26,** 1234-1255

Rahmstorf, S., 1999: Decadal variability of the thermohaline ocean circulation. In *Beyond El Niño Decadal and Interdecadal Climate Variability*, A. Navarra, ed., Springer.

Saenko, O.A., and A.J. Weaver, 2003: Southern ocean upwelling and eddies: sensitivity of the global overturning to the surface density range. Tellus, 55A, 106-111.

Schmitz, W.J., 1996: On the World Ocean Circulation I: Some Global Features/North Atlantic Circulation. WHOI Technical Report, WHOI-96-03.

Schmitz, W.J., 1996: On the World Ocean Circulation II: The Pacific and Indian Oceans/A Global Update WHOI Technical Report, WHOI-96-08.

Weaver, A.J., J. Marotzke, and E.S. Sarachik, 1991: Internal Low Frequency Variability of the Ocean's Thermohaline Circulation. *Nature*, **353**, 836-838.

Weaver, A.J., J. Marotzke, P.F. Cummins, and E.S. Sarachik 1993: Stability and variability of the thermohaline circulation. *J. Phys. Oceanogr.*,**23**, 39-60..

Winton, M. and E.S. Sarachik, 1993: Thermohaline oscillations of an oceanic general circulation model induced by strong steady salinity forcing. *J. Phys. Oceanogr.*, **23**, 1389-1410.

Winton, 1993: Deep decoupling oscillations of the oceanic thermohaline circulation. In *Ice in the Climate System*, W.R. Peltier, ed, Springer-Verlag.

Weaver, A.J., C.M. Bitz, A.F. Fanning and M.M. Holland, 1999: Thermohaline circulation: high latitude phenomena and the difference between the Pacific and Atlantic. *Ann. Rev.. Earth and Plan. Sci.* , **27**, 231-285.